rejuvenate the bioactivity and/or extend the life span of EPCs, can constitute such potential strategies.

We have recently shown for the first time that gene-modified EPCs rescue impaired neovascularization in an animal model of limb ischemia [57]. Transplantation of heterologous EPCs transduced with adenovirus encoding human VEGF165 not only improved neovascularization and blood flow recovery, but also had meaningful biological consequences, i.e. limb necrosis and auto-amputation were reduced by 63.7% in comparison with controls. Notably, the dose of EPCs needed to achieve limb salvage in these in vivo experiments was 30 times less than that required in the previous experiments involving unmodified EPCs [25]. Thus, combining EPC cell therapy with gene (i.e. VEGF) therapy may be one option to address the limited number and function of EPCs that can be isolated from peripheral blood in patients.

5.4. BM-MNC transplantation

Nonselected total BM cells or BM-MNCs including immature EPC population have also been investigated for their potential to induce neovascularization. Several experiments have reported that autologous BM administration into rabbit [58] or rat [59] hindlimb ischemic model, and porcine myocardial ischemic model [60,61] could augment neovascularization in ischemic tissue mainly through the production of angiogenic growth factors and less through the differentiation of a portion of the cells into EPCs/ECs in situ. Although there are no long-term safety and efficacy data for local delivery of such cell population mostly composed of inflammatory leukocytes, these strategies have already been applied to clinical patients in some institutions and preliminary results are expected soon.

6. Other devices of EPCs for clinical application

EPCs have recently been applied to the field of tissue engineering as a means of improving biocompatibility of vascular grafts. Artificial grafts first seeded with autologous CD34+ cells from canine BM and then implanted into the aortae were found to have increased surface endothelialization and vascularization compared with controls [62]. Similarly, when cultured autologous ovine EPCs were seeded onto carotid interposition grafts, the EPC-seeded grafts achieved physiological motility and remained patent for 130 days versus 15 days in non-seeded grafts [63]. Alternatively, as previously reported, the cell sheets of cultured cardiomyocytes may be effective for the improvement of cardiac function in the damaged hearts, i.e. ischemic heart disease or cardiomyopathy [64,65]. The cell sheets consisting of cardiomyocytes with EPCs expected to induce neovessels may be attractive, as blood supply is essential to maintain the homeostasis of implanted cardiomyocytes in such cell sheets.

EPCs have also been investigated in the cerebrovascular field. Embolization of the middle cerebral artery in Tie2/lacZ/BMT mice disclosed that the formation of new blood vessels in the adult brain after stroke involves vasculogenesis/EPCs [66]. Similar data were reported using gender-mismatched wild-type mice transplanted with BM from Green Fluorescein Protein transgenic mice [67]. However, whether autologous EPC transplantation would augment cerebral revascularization has yet to be examined.

To date, the role of EPCs in tumor angiogenesis has been demonstrated by several groups. Davidoff et al. showed that BM-derived EPCs contribute to tumor neovasculature and that BM cells transduced with an anti-angiogenic gene can restrict tumor growth in mice [45]. Lyden et al. recently used angiogenic defective, tumor resistant Id-mutant mice and showed the restoration of tumor angiogenesis with BM (donor)-derived EPCs throughout the neovessels following the transplantation of wild-type BM into these mice [46]. These data demonstrate that EPCs are not only important, but also critical, to tumor neovascularization. Given the findings, 'anti-tumor EPC mediated gene therapy' by transplantation of EPCs transferred genes to inhibit tumor growth may be developed in the near future.

Orlic et al. recently demonstrated that lineage marker negative (non-committed) and CD117 positive BM cells can regenerate de novo myocardium and ECs and improve cardiac function when they were locally delivered into murine myocardial infarction model [68]. They also reported that mobilization of BM cells by G-CSF and stem cell factor leads to a reduction in infarct size, improves cardiac function and decreases the mortality in this animal model [69]. Jackson et al. showed that BM-derived stem cells (side population cells defined by dye exclusion) can differentiate into cardiomyocytes and ECs at a very low rate in murine cardiac reperfusion injury model following BMT [70]. These studies suggest a clinical use of BM for cardiovascular diseases other than EPCs/therapeutic vasculogenesis. Given the extensive plasticity of BM cells differentiating into neural, hepatic and mesenchymal lineages, BM-derived EPCs may also exhibit such a potential, as seen in the report suggesting the transdifferentiation of endothelial lineage cells into cardiomyocytes [71].

7. Conclusion

As the concepts of BM-derived EPCs in adults and postnatal vasculogenesis are further established, clinical applications of EPCs to regenerative medicine are likely to follow. To acquire the more optimized quality and quantity of EPCs, several issues remain to be addressed, such as the development of a more efficient method of EPC purification and expansion, the methods of administration and senescence in EPCs. Alternatively, in the case of im-

possible utility of autologous BM-derived EPCs in the patients with impaired BM function, an appreciable number of EPCs isolated from umbilical cord blood or differentiated from tissue specific stem/progenitor or embryonic stem cells need to be optimized for EPC therapy. However, the unlimited potential of EPCs along with the emerging concepts of autologous cell therapy with gene modification suggests that they may soon reach clinical fruition.

Acknowledgements

We thank Y. Nakaya for secretarial assistance. Haruchika Masuda is the recipient of grants from the Kanagawa Nanbyo Foundation. Takayuki Asahara is the recipient of Grant-in-Aid 0051121T from the American Heart Association.

References

[1] Asahara T, Murohara T, Sullivan A et al. Isolation of putative progenitor endothelial cells for angiogenesis. Science 1997;275:964–967.
[2] Shi Q, Rafii S, Wu MH et al. Evidence for circulating bone marrow-derived endothelial cells. Blood 1998;92:362–367.
[3] Folkman J, Shing Y. Angiogenesis. J Biol Chem 1992;267:10931–10934.
[4] Asahara T, Masuda H, Takahashi T et al. Bone marrow origin of endothelial progenitor cells responsible for postnatal vasculogenesis in physiological and pathological neovascularization. Circ Res 1999;85:221–228.
[5] Tamaki T, Akatsuka A, Ando K et al. Identification of myogenic-endothelial progenitor cells in the interstitial spaces of skeletal muscle. J Cell Biol 2002;157:571–577.
[6] Gill M, Dias S, Hattori K et al. Vascular trauma induces rapid but transient mobilization of VEGFR2(+)AC133(+) endothelial precursor cells. Circ Res 2001;88:167–174.
[7] Shintani S, Murohara T, Ikeda H et al. Mobilization of endothelial progenitor cells in patients with acute myocardial infarction. Circulation 2001;103:2776–2779.
[8] Risau W, Sariola H, Zerwes HG et al. Vasculogenesis and angiogenesis in embryonic-stem-cell-derived embryoid bodies. Development 1988;102:471–478.
[9] Pardanaud L, Altmann C, Kitos P et al. Vasculogenesis in the early quail blastodisc as studied with a monoclonal antibody recognizing endothelial cells. Development 1987;100:339–349.
[10] Flamme I, Risau W. Induction of vasculogenesis and hematopoiesis in vitro. Development 1992;116:435–439.
[11] Weiss MJ, Orkin SH. In vitro differentiation of murine embryonic stem cells. New approaches to old problems. J Clin Invest 1996;97:591–595.
[12] Risau W, Flamme I. Vasculogenesis. Annu Rev Cell Dev Biol 1995;11:73–91.
[13] Choi K, Kennedy M, Kazarov A et al. A common precursor for hematopoietic and endothelial cells. Development 1998;125:725–732.
[14] Yin AH, Miraglia S, Zanjani ED et al. AC133, a novel marker for human hematopoietic stem and progenitor cells. Blood 1997;90:5002–5012.
[15] Peichev M, Naiyer AJ, Pereira D et al. Expression of VEGFR2 and AC133 by circulating human CD34(+) cells identifies a population of functional endothelial precursors. Blood 2000;95:952–958.
[16] Nieda M, Nicol A, Denning Kendall P et al. Endothelial cell precursors are normal components of human umbilical cord blood. Br J Haematol 1997;98:775–777.
[17] Murohara T, Ikeda H, Duan J et al. Transplanted cord blood-derived endothelial precursor cells augment postnatal neovascularization. J Clin Invest 2000;105:1527–1536.
[18] Kang HJ, Kim SC, Kim YJ et al. Short-term phytohaemagglutinin-activated mononuclear cells induce endothelial progenitor cells from cord blood CD34+ cells. Br J Haematol 2001;113:962–969.
[19] Crisa L, Cirulli V, Smith KA et al. Human cord blood progenitors sustain thymic T-cell development and a novel form of angiogenesis. Blood 1999;94:3928–3940.
[20] Crosby JR, Kaminski WE, Schatteman G et al. Endothelial cells of hematopoietic origin make a significant contribution to adult blood vessel formation. Circ Res 2000;87:728–730.
[21] Murayama T, Tepper OM, Silver M et al. Determination of bone marrow-derived endothelial progenitor cell significance in angiogenic growth factor-induced neovascularization in vivo. Exp Hematol 2002;30:967.
[22] Reyes M, Dudek A, Jahagirdar B et al. Origin of endothelial progenitors in human postnatal bone marrow. J Clin Invest 2002;109:337–346.
[23] Boyer M, Townsend LE, Vogel LM et al. Isolation of endothelial cells and their progenitor cells from human peripheral blood. J Vasc Surg 2000;31:181–189.
[24] Lin Y, Weisdorf DJ, Solovey A et al. Origins of circulating endothelial cells and endothelial outgrowth from blood. J Clin Invest 2000;105:71–77.
[25] Kalka C, Masuda H, Takahashi T et al. Transplantation of ex vivo expanded endothelial progenitor cells for therapeutic neovascularization. Proc Natl Acad Sci USA 2000;97:3422–3427.
[26] Gunsilius E, Duba HC, Petzer AL et al. Evidence from a leukaemia model for maintenance of vascular endothelium by bone-marrow-derived endothelial cells. Lancet 2000;355:1688–1691.
[27] Gehling UM, Ergun S, Schumacher U et al. In vitro differentiation of endothelial cells from AC133-positive progenitor cells. Blood 2000;95:3106–3112.
[28] Fernandez Pujol B, Lucibello FC et al. Endothelial-like cells derived from human CD14 positive monocytes. Differentiation 2000;65:287–300.
[29] Schatteman GC, Hanlon HD, Jiao C et al. Blood-derived angioblasts accelerate blood-flow restoration in diabetic mice. J Clin Invest 2000;106:571–578.
[30] Harraz M, Jiao C, Hanlon HD et al. CD34- blood-derived human endothelial cell progenitors. Stem Cells 2001;19:304–312.
[31] Quirici N, Soligo D, Caneva L et al. Differentiation and expansion of endothelial cells from human bone marrow CD133(+) cells. Br J Haematol 2001;115:186–194.
[32] Grzelak I, Olszewski WL, Zaleska M et al. Surgical trauma evokes a rise in the frequency of hematopoietic progenitor cells and cytokine levels in blood circulation. Eur Surg Res 1998;30:198–204.
[33] Takahashi T, Kalka C, Masuda H et al. Ischemia- and cytokine-induced mobilization of bone marrow-derived endothelial progenitor cells for neovascularization. Nat Med 1999;5:434–438.
[34] Shalaby F, Rossant J, Yamaguchi TP et al. Failure of blood-island formation and vasculogenesis in Flk-1-deficient mice. Nature 1995;376:62–66.
[35] Carmeliet P, Ferreira V, Breier G et al. Abnormal blood vessel development and lethality in embryos lacking a single VEGF allele. Nature 1996;380:435–439.
[36] Ferrara N, Carver Moore K et al. Heterozygous embryonic lethality induced by targeted inactivation of the VEGF gene. Nature 1996;380:439–442.
[37] Asahara T, Takahashi T, Masuda H et al. VEGF contributes to postnatal neovascularization by mobilizing bone marrow-derived endothelial progenitor cells. EMBO J 1999;18:3964–3972.

[38] Kalka C, Masuda H, Takahashi T et al. Vascular endothelial growth factor(165) gene transfer augments circulating endothelial progenitor cells in human subjects. Circ Res 2000;86:1198–1202.
[39] Moore MA, Hattori K, Heissig B et al. Mobilization of endothelial and hematopoietic stem and progenitor cells by adenovector-mediated elevation of serum levels of SDF-1, VEGF, and angiopoietin-1. Ann NY Acad Sci 2001;938:36–45; discussion 45–47.
[40] Kureishi Y, Luo Z, Shiojima I et al. The HMG-CoA reductase inhibitor simvastatin activates the protein kinase Akt and promotes angiogenesis in normocholesterolemic animals. Nat Med 2000;6:1004–1010.
[41] Llevadot J, Murasawa S, Kureishi Y et al. HMG-CoA reductase inhibitor mobilizes bone marrow-derived endothelial progenitor cells. J Clin Invest 2001;108:399–405.
[42] Dimmeler S, Aicher A, Vasa M et al. HMG-CoA reductase inhibitors (statins) increase endothelial progenitor cells via the PI 3-kinase/Akt pathway. J Clin Invest 2001;108:391–397.
[43] Vasa M, Fichtlscherer S, Adler K et al. Increase in circulating endothelial progenitor cells by statin therapy in patients with stable coronary artery disease. Circulation 2001;103:2885–2890.
[44] Urbich C, Dernbach E, Zeiher AM et al. Double-edged role of statins in angiogenesis signaling. Circ Res 2002;90:737–744.
[45] Davidoff AM, Ng CY, Brown P et al. Bone marrow-derived cells contribute to tumor neovasculature and, when modified to express an angiogenesis inhibitor, can restrict tumor growth in mice. Clin Cancer Res 2001;7:2870–2879.
[46] Lyden D, Hattori K, Dias S et al. Impaired recruitment of bone-marrow-derived endothelial and hematopoietic precursor cells blocks tumor angiogenesis and growth. Nat Med 2001;7:1194–1201.
[47] Rivard A, Silver M, Chen D et al. Rescue of diabetes-related impairment of angiogenesis by intramuscular gene therapy with adeno-VEGF. Am J Pathol 1999;154:355–363.
[48] Van Belle E, Rivard A, Chen D et al. Hypercholesterolemia attenuates angiogenesis but does not preclude augmentation by angiogenic cytokines. Circulation 1997;96:2667–2674.
[49] Couffinhal T, Silver M, Kearney M et al. Impaired collateral vessel development associated with reduced expression of vascular endothelial growth factor in ApoE−/− mice. Circulation 1999;99:3188–3198.
[50] Rivard A, Berthou Soulie L, Principe N et al. Age-dependent defect in vascular endothelial growth factor expression is associated with reduced hypoxia-inducible factor 1 activity. J Biol Chem 2000;275:29643–29647.
[51] Rivard A, Fabre JE, Silver M et al. Age-dependent impairment of angiogenesis. Circulation 1999;99:111–120.
[52] Murayama T, Kalka C, Silver M et al. Aging impairs therapeutic contribution of human endothelial progenitor cells to postnatal neovascularization [Abstract]. Circulation 2001;104:II-68.
[53] Vasa M, Fichtlscherer S, Aicher A et al. Number and migratory activity of circulating endothelial progenitor cells inversely correlate with risk factors for coronary artery disease. Circ Res 2001;89:E1–E7.
[54] Kawamoto A, Gwon HC, Iwaguro H et al. Therapeutic potential of ex vivo expanded endothelial progenitor cells for myocardial ischemia. Circulation 2001;103:634–637.
[55] Kocher AA, Schuster MD, Szabolcs MJ et al. Neovascularization of ischemic myocardium by human bone-marrow-derived angioblasts prevents cardiomyocyte apoptosis, reduces remodeling and improves cardiac function. Nat Med 2001;7:430–436.
[56] Levenberg S, Golub JS, Amit M et al. Endothelial cells derived from human embryonic stem cells. Proc Natl Acad Sci USA 2002;99:4391–4396.
[57] Iwaguro H, Yamaguchi J, Kalka C et al. Endothelial progenitor cell vascular endothelial growth factor gene transfer for vascular regeneration. Circulation 2002;105:732–738.
[58] Shintani S, Murohara T, Ikeda H et al. Augmentation of postnatal neovascularization with autologous bone marrow transplantation. Circulation 2001;103:897–903.
[59] Hamano K, Li TS, Kobayashi T et al. The induction of angiogenesis by the implantation of autologous bone marrow cells: a novel and simple therapeutic method. Surgery 2001;130:44–54.
[60] Kamihata H, Matsubara H, Nishiue T et al. Implantation of bone marrow mononuclear cells into ischemic myocardium enhances collateral perfusion and regional function via side supply of angioblasts, angiogenic ligands, and cytokines. Circulation 2001;104:1046–1052.
[61] Fuchs S, Baffour R, Zhou YF et al. Transendocardial delivery of autologous bone marrow enhances collateral perfusion and regional function in pigs with chronic experimental myocardial ischemia. J Am Coll Cardiol 2001;37:1726–1732.
[62] Bhattacharya V, McSweeney PA, Shi Q et al. Enhanced endothelialization and microvessel formation in polyester grafts seeded with CD34(+) bone marrow cells. Blood 2000;95:581–585.
[63] Kaushal S, Amiel GE, Guleserian KJ et al. Functional small-diameter neovessels created using endothelial progenitor cells expanded ex vivo. Nat Med 2001;7:1035–1040.
[64] Shimizu T, Yamato M, Isoi Y et al. Fabrication of pulsatile cardiac tissue grafts using a novel 3-dimensional cell sheet manipulation technique and temperature-responsive cell culture surfaces. Circ Res 2002;90:e40.
[65] Shimizu T, Yamato M, Akutsu T et al. Electrically communicating three-dimensional cardiac tissue mimic fabricated by layered cultured cardiomyocyte sheets. J Biomed Mater Res 2002;60:110–117.
[66] Zhang ZG, Zhang L, Jiang Q et al. Bone marrow-derived endothelial progenitor cells participate in cerebral neovascularization after focal cerebral ischemia in the adult mouse. Circ Res 2002;90:284–288.
[67] Hess DC, Hill WD, Martin Studdard A et al. Bone marrow as a source of endothelial cells and NeuN-expressing cells after stroke. Stroke 2002;33:1362–1368.
[68] Orlic D, Kajstura J, Chimenti S et al. Bone marrow cells regenerate infarcted myocardium. Nature 2001;410:701–705.
[69] Orlic D, Kajstura J, Chimenti S et al. Mobilized bone marrow cells repair the infarcted heart, improving function and survival. Proc Natl Acad Sci USA 2001;98:10344–10349.
[70] Jackson KA, Majka SM, Wang H et al. Regeneration of ischemic cardiac muscle and vascular endothelium by adult stem cells. J Clin Invest 2001;107:1395–1402.
[71] Condorelli G, Borello U, De Angelis L et al. Cardiomyocytes induce endothelial cells to trans-differentiate into cardiac muscle: implications for myocardium regeneration. Proc Natl Acad Sci USA 2001;98:10733–10738.

Stromal Cell–Derived Factor-1 Effects on Ex Vivo Expanded Endothelial Progenitor Cell Recruitment for Ischemic Neovascularization

Jun-ichi Yamaguchi, MD, PhD; Kengo Fukushima Kusano, MD, PhD; Osamu Masuo, MD; Atsuhiko Kawamoto, MD, PhD; Marcy Silver, BS; Satoshi Murasawa, MD, PhD; Marta Bosch-Marce, PhD; Haruchika Masuda, MD, PhD; Douglas W. Losordo, MD; Jeffrey M. Isner, MD†; Takayuki Asahara, MD, PhD

Background—Stromal cell–derived factor-1 (SDF-1) is a chemokine considered to play an important role in the trafficking of hematopoietic stem cells. Given the close relationship between hematopoietic stem cells and endothelial progenitor cells (EPCs), we investigated the effect of SDF-1 on EPC-mediated vasculogenesis.

Methods and Results—Flow cytometric analysis demonstrated expression of CXCR4, the receptor of SDF-1, by 66±3% of EPCs after 7 days in culture. In vitro modified Boyden chamber assay showed a dose-dependent EPC migration toward SDF-1 (control versus 10 ng/mL SDF-1 versus 100 ng/mL SDF-1, 24±2 versus 71±3 versus 140±6 cells/mm^2; $P<0.0001$). SDF-1 attenuated EPC apoptosis (control versus SDF-1, 27±1 versus 7±1%; $P<0.0001$). To investigate the effect of SDF-1 in vivo, we locally injected SDF-1 into athymic ischemic hindlimb muscle of nude mice combined with human EPC transplantation to determine whether SDF-1 augmented EPC-induced vasculogenesis. Fluorescence microscopic examination disclosed increased local accumulation of fluorescence-labeled EPCs in ischemic muscle in the SDF-1 treatment group (control versus SDF-1=241±25 versus 445±24 cells/mm^2, $P<0.0001$). At day 28 after treatment, ischemic tissue perfusion was improved in the SDF-1 group and capillary density was also increased. (control versus SDF-1, 355±26 versus 551±30 cells/mm^2; $P<0.0001$).

Conclusion—These findings indicate that locally delivered SDF-1 augments vasculogenesis and subsequently contributes to ischemic neovascularization in vivo by augmenting EPC recruitment in ischemic tissues. **(*Circulation*. 2003;107: 1322-1328.)**

Key Words: chemokines ■ angiogenesis ■ ischemia ■ endothelium

Stromal cell–derived factor-1 (SDF-1) is a member of the chemokine CXC subfamily originally isolated from murine bone marrow stromal cells.[1] It has a single substantial open reading frame of 267 nucleotides encoding an 89-amino acid polypeptide and expressed on stromal cells of various tissues. On the other hand, CXCR4, a 7-transmembrane-spanning G protein–coupled receptor, is the only known receptor for SDF-1 and is also a coreceptor for HIV type 1 infection.[2] SDF-1/CXCR4 interaction is reported to play an important physiological role during embryogenesis in hematopoiesis,[3] vascular development, cardiogenesis,[4] and cerebellar development.[5]

Recently, several investigators reported that CD34$^+$ cells, classically considered to be hematopoietic stem cells, expressed CXCR4, and that SDF-1 could induce CD34$^+$ cell migration in vitro.[6] Accordingly, SDF-1 is considered as one of the key regulators of hematopoietic stem cell trafficking between the peripheral circulation and bone marrow. SDF-1 has also been shown to effect CD34$^+$ cell proliferation[7] and mobilization[8] and to induce angiogenesis in vivo.[9]

Bone marrow–derived endothelial progenitor cells (EPCs) have been isolated from the peripheral blood of adult species.[10,11] These cells participate in not only physiological but also pathological neovascularization in response to certain cytokines and/or tissue ischemia.[12–14] More recently, ex vivo expanded EPCs from peripheral blood, transplanted into animal models of ischemic hindlimbs and acute myocardial infarction, successfully augmented neovascularization resulting in physiological recovery documented as limb salvage and improvement in myocardial function.[15,16]

Received August 12, 2002; revision received December 5, 2002; accepted December 5, 2002.

From the Division of Cardiovascular Research and Medicine (J.Y., K.F.K., O.M., A.K., M.S., S.M., M.B.M., D.W.L., J.M.I., T.A.), St Elizabeth's Medical Center, Tufts University School of Medicine, Boston, Mass, and Department of Physiology (H.M., T.A.), Tokai University School of Medicine, Tokai, Japan.

†Deceased.

Correspondence to Takayuki Asahara, MD, PhD, or Douglas W. Losordo, MD, Division of Cardiovascular Research and Medicine, St Elizabeth's Medical Center, 736 Cambridge St, Boston, MA, 02135. E-mail asa777@aol.com (T.A.) or douglas.losordo@tufts.edu

© 2003 American Heart Association, Inc.

Circulation is available at http://www.circulationaha.org

DOI: 10.1161/01.CIR.0000055313.77510.22

At present, however, enthusiasm for the therapeutic potential of strategies of EPC transplantation is limited by certain practical considerations. For example, adjusting the number of EPCs for injection according to body weight, ≈6 L of blood would be required for harvesting of EPCs in an average-size patient to administer a dose equivalent to that which yielded therapeutic effects in limb and myocardial ischemia in small animal models. Accordingly, we investigated the hypothesis that locally administered SDF-1 could augment the local accumulation of transplanted EPCs, thereby resulting in enhanced neovascularization. Here we report that EPCs express CXCR4 and that the combination of SDF-1 local administration and EPC transplantation has potential as a strategy for therapeutic neovascularization.

Methods

Cell Isolation and Culture

Ex vivo expansion of EPCs was performed as described.[10] In brief, total human peripheral blood mononuclear cells were isolated from healthy human volunteers by density-gradient centrifugation with Histopaque-1077 (Sigma) and plated on culture dishes coated with human fibronectin (Sigma). The cells were cultured in endothelial cell basal medium-2 (EBM-2, Clonetics) supplemented with 5% FBS, human vascular endothelial growth factor (VEGF)-A, human fibroblast growth factor-2, human epidermal growth factor, insulin-like growth factor-1, ascorbic acid, and antibiotics. After 4 days in culture, nonadherent cells were removed by washing with PBS, new medium was applied, and the culture was maintained through day 7.

$CD34^+$ cells from isolated human peripheral blood mononuclear cells were positively selected using the MiniMACS immunomagnetic separation system (Milteney Biotec) according to the manufacturer's instructions as recently described.[7]

Fluorescence-Activated Cell Sorting

Fluorescence-activated cell sorting (FACS) detection of EPCs was performed after 7 days in culture. The procedure of FACS staining was described previously.[16] In brief, a total of 2 to 3×10^5 cells were resuspended with 200 μL of Dulbecco's PBS (BioWhittaker) containing 10% FBS and 0.01% NaN_3 and incubated for 20 minutes at 4°C with phycoerythrin-conjugated monoclonal antibodies against CXCR4 (PharMingen). After staining, the cells were fixed in 2% paraformaldehyde. Quantitative FACS was performed on a FACStar flow cytometer (Becton Dickinson). All groups were studied at least in triplicate.

Migration Assay

To investigate EPC migration activity, a modified Boyden chamber assay was performed using a 48-well microchemotaxis chamber (NeuroProbe) as described.[17] In brief, SDF-1 (PharMingen) is diluted to appropriate concentrations in EBM-2 supplemented with 0.1% BSA, and 30 μL of the final dilution was placed in the lower compartment of a Boyden chamber. Human EPCs cultured for 7 days were harvested, 3×10^4 cells were suspended in 50 μL of EBM-2 supplemented with 0.1% BSA, and antibiotics were reseeded in the upper compartment. After incubation for 5 hours at 37°C, the filter was removed, and the cells on the filter were counted manually in random high-power fields (×100) in each well. All groups were studied at least in triplicate.

Apoptosis Assay

EPC apoptosis, induced by serum starvation, was quantified to determine whether SDF-1 exerts a survival effect on EPCs. The proportion of apoptotic EPCs after serum starvation was determined by manually counting pyknotic nuclei after DAPI (Roche) staining. In brief, day 7 EPCs were reseeded onto 4-chamber slides (1×10^5 cells per well with 500 μL of EPC culture medium). After 24 hours of incubation, culture medium was removed and replaced with 500 μL of EBM-2 without any supplement. After 48 hours of serum deprivation, the medium was supplemented with 100 ng/mL of SDF-1 (versus medium alone) and incubated for 3 hours. DAPI-stained pyknotic nuclei were counted as percentage of 100 cells in each well. Each group was studied at least in triplicate.

Animal Model of Ischemic Hindlimb

All procedures were performed in accordance with the Institutional Animal Care and Use Committee of St Elizabeth's Medical Center. Male athymic nude mice (CBy-Cg-Foxnl^{nu}, The Jackson Laboratory), age 8 to 10 weeks and weighing 18 to 22 g, were anesthetized with sodium pentobarbital (160 mg/kg IP) for operative resection of one femoral artery as described.[16] For euthanization, mice were injected with an overdose of pentobarbital.

RNA Extraction and Reverse Transcriptase–Polymerase Chain Reaction Analysis

Tissue RNA was extracted from frozen muscle samples (day 7 after hindlimb ischemia) using TRIzol reagent (Invitrogen) according to the manufacturer's instructions. Reverse transcriptase–polymerase chain reaction (RT-PCR) of the VEGF and GAPDH genes was performed using 1 μg of total RNA. PCR was performed for 35 cycles for VEGF-A and 25 cycles for GAPDH, with each cycle consisting of 94°C for 30 seconds and 64°C for 3 minutes. Amplification was carried out in 20-μL reaction mixtures containing 0.4 U *Taq* polymerase.

Transplantation of Ex Vivo Expanded EPCs

The impact of local administration of SDF-1 after EPC transplantation on therapeutic neovascularization was investigated in a murine model of hindlimb ischemia.[16] Just after operative excision of one femoral artery, athymic nude mice, described above, in which angiogenesis is characteristically impaired, received a local intramuscular injection of 1 μg SDF-1 versus PBS in the center of the lower calf muscle followed immediately by an intravenous injection of 1.5×10^5 culture-expanded EPCs. To evaluate EPC incorporation into the vasculature in ischemic muscles, some mice were transplanted with EPCs labeled with the fluorescent carbocyanine 1,1′-dioctadecyl-1 to 3,3,3′3′-tetramethylidocarboyanine perchlorate (DiI) dye (Molecular Probes). Before transplantation, EPCs in suspension were washed with PBS and incubated with DiI at a concentration of 2.5 μg/mL PBS for 5 minutes at 37°C and 15 minutes at 4°C. After 2 washing steps in PBS, the cells were resuspended in EBM-2. Five mice in the placebo and SDF-1 groups each received 1.5×10^5 DiI-labeled EPCs intravenously as described above. Thirty minutes before euthanization at day 3 and day 7, 5 mice in each group received an intravenous injection of 50 μg of *Bandeiraea simplicifolia* lectin 1 (BS-1 lectin, Vector Laboratories) to identify the mouse vasculature.

Physiological Assessment of Transplanted Animals

Laser Doppler perfusion imaging (LDPI, Moor Instruments) was used to record serial blood flow measurements over the course of 4 weeks postoperatively, as previously described.[16] There were 8 mice in the SDF-1 group and 9 in the PBS group. In these digital color-coded images, a red hue indicates the region of maximum perfusion, medium perfusion values are shown in yellow, and the lowest perfusion values are represented by blue. Figure 5B displays absolute values in readable units.

Histological Assessment of Transplanted Animals

Tissue sections from the lower calf muscles of ischemic and healthy limbs were harvested on days 3, 7, and 28. To examine EPC incorporation at early time points after transplantation (at days 3 and 7) and SDF-1 effect on host endothelial cells, tissues from the mice injected with DiI-labeled EPCs and BS-1 lectin were embedded for frozen section samples. A total of 20 different fields (4 cross sections from each animal) were randomly selected, and the DiI-labeled EPCs were counted (×40 magnification).

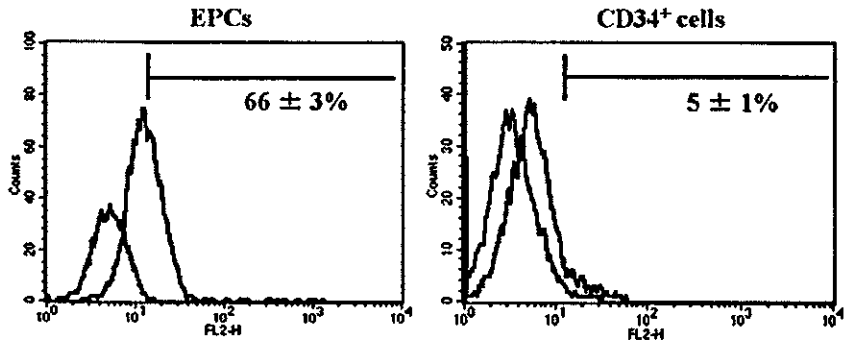

Figure 1. Analysis of CXCR-4 expression by flow cytometry. Results are shown as fluorescence histograms (blue, CXCR-4 expression; red, respective IgG control). Ex vivo expanded EPCs were positive by 66.0±3.1% for CXCR-4, and freshly isolated peripheral blood CD34+ cells by 5.2±1.1%. FL2-H indicates fluorescent intensity.

The extent of neovascularization at day 28 was assessed by measuring capillary density in light microscopic sections.[16] Paraffin-embedded sections of 5-μm thickness were stained for the mouse endothelial cell marker isolectin B4 (Vector Laboratories) and counterstained with eosin to detect capillary endothelial cells as previously described.[15] A total of 20 different fields were randomly selected (2 or 3 cross sections from each animal), and the capillaries were counted (×40 magnification).

Statistical Analysis

All results are expressed as mean±SEM. Statistical significance was evaluated using the unpaired Student *t* test for comparisons between 2 means. Multiple comparisons between >3 groups were done by ANOVA. Probability value of $P<0.05$ denoted statistical significance.

Results

Fluorescence-Activated Cell Sorting

After 7 days of culture, ex vivo expanded EPCs derived from peripheral blood of healthy human volunteers exhibited spindle-shaped morphology. These progenitor cells have qualitative properties of endothelial lineage cells.[16] FACS analysis elucidated that 66.0±3.1% of day 7 cultured EPCs express CXCR4, whereas only 5.2±1.1% of freshly isolated human peripheral blood CD34+ cells showed CXCR4 expression (Figure 1). In addition, 50.6±4.7% of CD34+ cells cultured 24 hours with EPC culture medium expressed CXCR4, which is consistent with previous reports.[7]

Migration Assay

To investigate the migratory response of ex vivo expanded EPCs toward an SDF-1, we performed a modified Boyden chamber assay in vitro. SDF-1 induced EPC migration in a dose-dependent manner (Figure 2). The magnitude of migration was similar to that induced by VEGF (data not shown). SDF-1 induced a small, statistically insignificant increase in EPC proliferative activity (data not shown).

Apoptosis Assay

To examine the effect of SDF-1 on ex vivo expanded EPC survival, we quantified apoptosis induced by serum starvation. After 48 hours of serum starvation, ex vivo expanded EPCs were treated with 100 ng/mL of SDF-1 for 3 hours. DAPI staining was performed to determine the proportion of apoptotic cells by manually counting pyknotic nuclei (Figure 3A). SDF-1 reduced apoptosis of EPCs from 26.6±1.0% to 7.1±0.9% ($P<0.0001$) (Figure 3B).

SDF-1 Upregulates Endogenous VEGF Expression in Hindlimb Ischemic Muscle

To investigate whether SDF-1 upregulates endogenous VEGF expression, we examined the expression of VEGF-A in the hindlimb ischemic muscle. Figure 4A shows temporal expression of VEGF-A mRNA in hindlimb muscle from mice treated with SDF-1 or PBS. Seven days after the treatment, VEGF-A mRNA expression was increased in SDF-1–treated muscle. Quantitative analysis of expression is shown in Figure 4B.

EPC Incorporation Into Ischemic Hindlimb Neovasculature

To elucidate the SDF-1 effect on local recruitment of transplanted EPCs from the systemic circulation and of host endothelial cells, we quantified incorporation of transplanted EPCs into the microvasculature of ischemic limbs and the number of host endothelial cells after local SDF-1 administration in nude mice hindlimbs. Transplanted human EPCs labeled with DiI were identified in tissue sections by red fluorescence, whereas the native mouse vasculature stained by premortem BS-1 lectin administration was identified by green fluorescence in the same tissue sections (Figure 5A). Histological examination disclosed increased local accumulation of DiI-labeled EPCs in the SDF-1 group compared with PBS controls (day 3, 445±24 versus 241±25 cells/mm^2, $P<0.0001$; day 7, 446±31 versus 355±30 cells/mm^2,

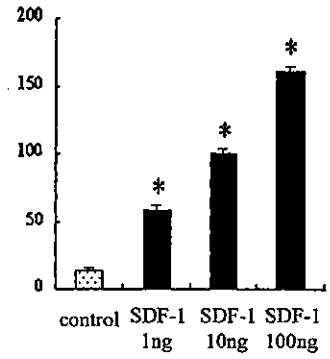

Figure 2. SDF-1 induced EPC migration. Migratory response of EPCs toward different dosages of SDF-1 stimulation was measured by modified Boyden chamber migration assay. Ex vivo expanded EPCs demonstrated a potent dose-dependent activity toward SDF-1. Control vs 10 ng/mL SDF-1 vs 100 ng/mL SDF-1, 24±2 vs 71±3 vs 140±6 cells/mm^2; *$P<0.0001$.

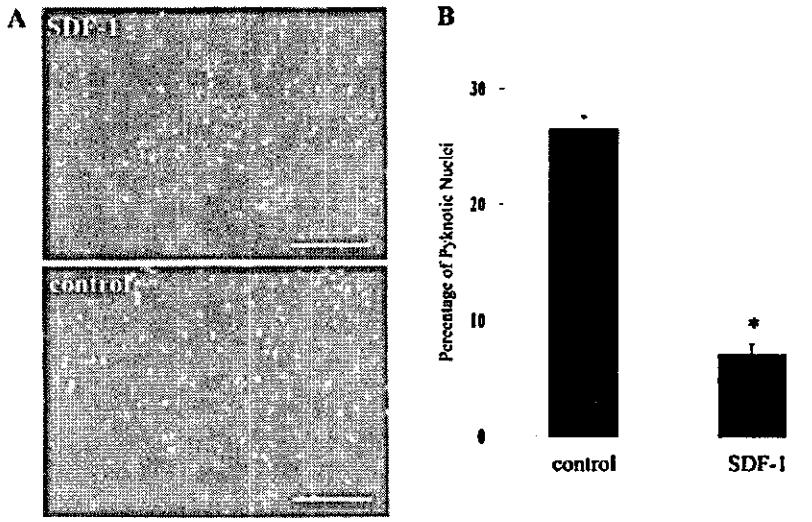

Figure 3. SDF-1 attenuated EPCs apoptosis. Serum starvation was used to induce apoptosis in ex vivo expanded EPCs. A, DAPI staining was performed to determine the proportion of apoptotic cells by manually counting pyknotic nuclei (white condensed nuclei in figures). Scale bars=100 μm. B, Quantification of percentage of pyknotic nuclei. Control vs SDF-1, 27±1% vs 7±1%; *$P<0.0001$.

$P<0.05$) (Figure 5B). Moreover, increased numbers of host endothelial cells were observed in the SDF-1 group compared with the PBS group (day 3, 500±19 versus 343±23 cells/mm^2, $P<0.0001$; day 7, 531±19 versus 386±25 cells/mm^2, $P<0.05$) (Figure 5C).

Physiological Assessment of Transplanted Animals

After systemic human EPC transplantation with local intramuscular administration of SDF-1 or PBS, serial measurements of hindlimb perfusion by LDPI were performed at days 7, 14, 21, and 28. LDPI disclosed profound differences in the limb perfusion 28 days after induction of limb ischemia (Figure 6A). By day 28, the ratio of ischemic/nonischemic blood flow in the SDF-1 treatment group improved to 0.50±0.08 versus 0.26±0.04 in the PBS group ($P<0.05$, Figure 6B). Thus, the homing effect of local SDF-1 injection documented above was accompanied by physiological evidence for enhanced neovascularization, suggesting that the EPCs that were attracted to the ischemic limb by SDF-1 were subsequently incorporated into the developing vasculature. To provide anatomic evidence of EPC-increased vasculature in the SDF-1–treated limbs, histological examination for capillary density was performed.[16]

Histological Assessment of Transplanted Animals

Staining with the endothelial cell marker isolectin B4 was performed on skeletal muscle sections retrieved from the ischemic hindlimbs of mice at day 28 to quantify capillary density (Figure 7A). Capillary density, an index of neovascularization, was significantly higher in the SDF-1 treatment group (551±30 cells/mm^2) than in the PBS treatment group (241±25 cells/mm^2, $P<0.0001$) (Figure 7B).

Discussion

Our previous studies indicated that ex vivo cell therapy, consisting of systemic implantation of culture-expanded hu-

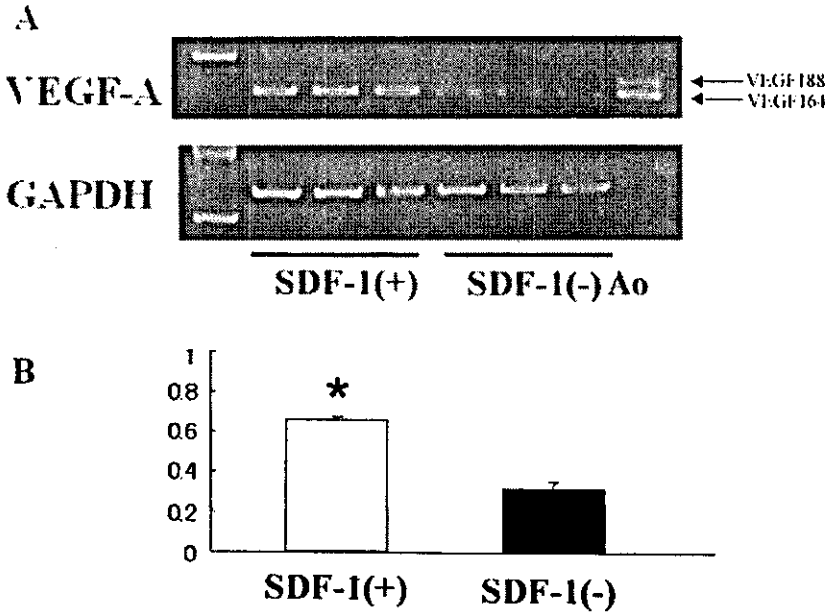

Figure 4. SDF-1 upregulated expression of VEGF-A mRNA in ischemic hindlimb. A, Expression of VEGF-A mRNA in SDF-1–treated and untreated muscle. Each panel shows RT-PCR products for VEGF-A and GAPDH. Ao indicates mouse aortic tissue as positive control. B, Densitometric analysis was performed; ratio of RT-PCR product of VEGF-A ($VEGF_{164}$) to that of GAPDH is shown. Data were obtained from 3 separate experiments and are presented as arbitrary units over controls. *$P<0.01$ (unpaired t test) vs SDF-1 (−) group.

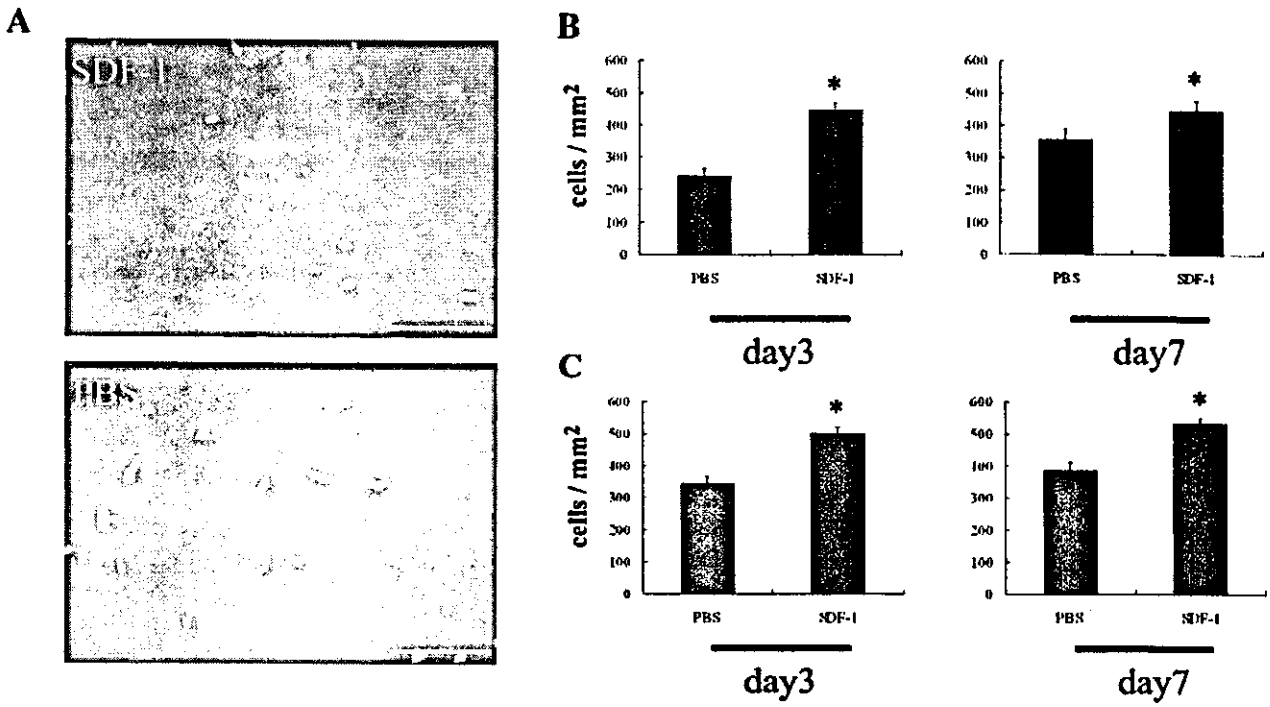

Figure 5. SDF-1 augmented EPC incorporation at an early time point. Fluorescence microscopic examination disclosed increased local accumulation of EPCs in SDF-1 treatment group compared with PBS group. A, Representative microscopic photographs of double fluorescence in ischemic muscles at day 3. Transplanted human DiI-labeled EPC-derived cells were identified by red fluorescence in histological sections retrieved from ischemic muscles. Host mouse vasculature was identified by green fluorescence in the same tissue sections. Scale bars=100 μm. B, Quantitative analysis of incorporated EPCs. Density of DiI-labeled EPCs (red fluorescence) in tissue sections retrieved from ischemic muscles was greater in SDF-1 treatment group than in PBS group at both days 3 and 7 (day 3, control vs SDF-1, 241±25 vs 445±24 cells/mm², *P<0.0001; day 7, control vs SDF-1, 355±30 vs 446±31 cells/mm², *P<0.05). C, Quantitative analysis of host endothelial cells. Density of host endothelial cells (green fluorescence) in tissue sections retrieved from ischemic muscles was greater in SDF-1 treatment group than in PBS group at both days 3 and 7 (day 3, control vs SDF-1, 343±23 vs 500±19 cells/mm², *P<0.0001; day 7, control vs SDF-1, 386±25 vs 531±19 cells/mm², *P<0.05).

man EPCs, successfully promotes neovascularization of ischemic hindlimbs[16] and acute myocardial infarction[15] in immune-deficient animal models. In these studies, heterogenous cell transplantation not only improved neovascularization but also reduced adverse biological consequences such as limb necrosis and autoamputation in the mouse ischemic hindlimb model. These studies also disclosed that systemic EPC transplantation improved myocardial neovascularization and cardiac function corresponding to reduced left ventricular scarring.

SDF-1 Effect on Vasculogenesis

Recent reports[6,7] indicated that SDF-1 was a strong chemoattractant for CD34$^+$ cells, which express CXCR4, the receptor for SDF-1, and played an important role in hematopoietic stem cell trafficking between the peripheral circulation and bone marrow. In addition, certain evidence suggests that SDF-1 may have direct effects on vasculogenesis. Tachibana et al[4] reported that mice lacking SDF-1 had defective formation of large vessels supplying the gastrointestinal tract. More recently, Hattori et al[8] reported that plasma elevation of SDF-1 induced mobilization of mature and immature hematopoietic progenitors and stem cells, including EPCs.

SDF-1 Contributes to Neovascularization by Augmenting Local Accumulation of Transplanted EPCs in Ischemic Tissues

Given the close relationship between hematopoietic stem cells and EPCs, we focused on the chemoattractant properties of SDF-1. We investigated the hypothesis that locally administered SDF-1 might augment the accumulation of EPCs to the site of ischemia, resulting in enhancing the efficacy of neovascularization after systemic EPC transplantation. The factors mediating the recruitment of circulating progenitors to ischemic tissue are not well characterized. Western analysis detected no SDF-1 protein in ischemic muscles (data not shown). We hypothesized that exogenous SDF-1, administered into ischemic tissue, could exert a strong chemoattractant effect for circulating EPCs, augmenting the effect of endogenous angiogenic/chemoattractant factors.

Our in vitro data verified the feasibility of this approach. CXCR4, the receptor for SDF-1, is expressed by EPCs, and the percentage of EPCs expressing CXCR4 was 13-fold higher compared with that of freshly isolated peripheral blood-derived CD34$^+$ cells. SDF-1 induced EPC migration and also exerted a survival effect on cultured EPCs.

In vivo, local SDF-1 administration augmented EPC accumulation 3 days after the treatment, which is consistent with

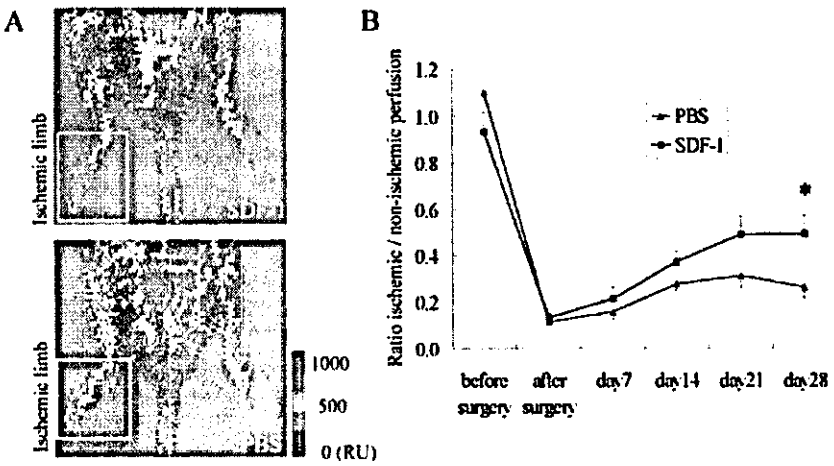

Figure 6. SDF-1 improved tissue perfusion. Hindlimb perfusion was measured by LDPI. A, Representative LDPI 28 days after induction of limb ischemia. Boxes indicate areas of interest. B, Quantitative analysis of perfusion recovery measured by LDPI. Ratios of ischemic/nonischemic limbs at day 28 were as follows: for PBS, 0.26±0.04; for SDF-1, 0.50±0.08; *$P<0.05$.

a chemoattractant effect in excess of the native locally expressed factors. The magnitude of EPC incorporation in the SDF-1 treatment group at day 3 was 1.8-fold higher than in the control group. The magnitude of EPC incorporation was similar between days 3 and 7, suggesting that the homing of exogenously administered EPCs occurs early after transplantation. Subsequent physiological and histological evaluations were performed to determine whether this increase in EPC local accumulation culminated in an increase in neovascularization. Serial LDPI measurements indicated significant differences in limb perfusion 28 days after induction of ischemia, whereas histological analysis revealed that capillary density, a direct anatomic reflection of neovascularization, was significantly greater in the SDF-1 treatment group than in the control group. These data provide evidence that the ultimate degree of physiological improvement is critically dependent on sufficient EPC recruitment at an early time point.[18,19]

It seems likely that in addition to transplanted EPCs, SDF-1 might stimulate host endothelial cells from preexisting blood vessels and host EPCs derived from bone marrow. Indeed, Salcedo et al[9] reported that subcutaneous serial SDF-1 injections into mouse skin induced formation of local small blood vessels and that SDF-1 treatment enhanced VEGF release from human umbilical vein endothelial cells in vitro. We have also observed enhanced VEGF release from EPCs treated with SDF-1 in vitro (data not shown).[20] Taken together with these observations, SDF-1 appears to have effects on endogenous angiogenesis (direct or via certain secondary cytokines) as well as vasculogenesis.

However, SDF-1 administered locally as the sole therapy for hindlimb ischemia in the same animal model resulted in autoamputation within 7 days in all animals (n=5, data not shown). Accordingly, at least under the experimental conditions used in this study, the effect of SDF-1 on neovascularization appears to result primarily from its ability to enhance the recruitment and incorporation of transplanted EPCs.

To the best of our knowledge, this study represents the first experimental proof of principle for the feasibility and therapeutic effectiveness of augmenting local accumulation of EPCs. EPCs widely express CXCR4, and local administration of SDF-1 enhanced vasculogenesis and subsequently contributed to neovascularization in vivo inducing in situ recruitment of transplanted EPCs in ischemic tissues. To apply SDF-1 treatment in clinical ischemic patients, certain issues will need to be considered, such as the effect of SDF-1 on atherosclerosis. Additional experiments using atherosclerotic animal models may shed light on this concern. Nevertheless, we believe that the concept of augmenting local accumulation of transplanted EPCs opens perspectives for the clinical strategy of EPC therapies.

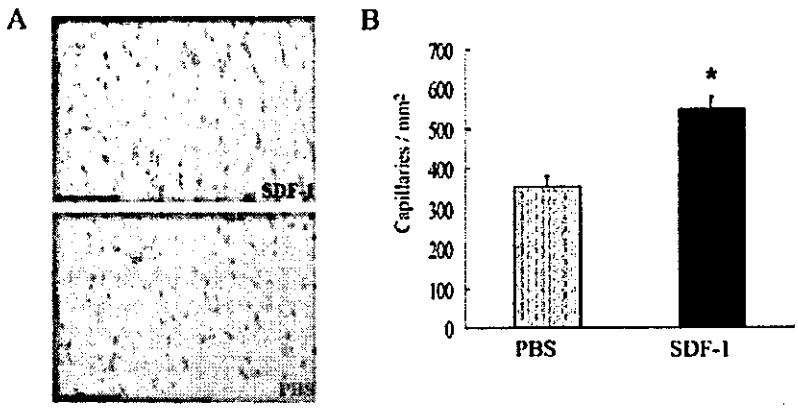

Figure 7. SDF-1 increased capillary density in ischemic tissue at day 28. Histological skeletal muscle section retrieved from ischemic hindlimbs at day 28 was examined for capillary density, an index of neovascularization, using endothelial-specific chemical staining of isolectin B4. A, Representative microscopic photographs of isolectin B4 histochemical staining in ischemic muscles at day 28. Brown indicates isolectin B4–positive vasculatures. Scale bars=100 μm. B, Quantitative analysis of capillary density. PBS vs SDF-1, 355±26 vs 551±30 cells/mm^2 (*$P<0.0001$).

Acknowledgments

This research is supported in part by National Institutes of Health Grants HL57516, HL60911, and HL53354; a Grant-in-Aid from the American Heart Association (to Takayuki Asahara); and a Grant-in-Aid from the Uehara Memorial Foundation (to Jun-ichi Yamaguchi).

This article is dedicated to Dr Jeffrey M. Isner, who died on October 31, 2001. We gratefully acknowledge him for his inspirational leadership, friendship, and encouraging support.

References

1. Nagasawa T, Kikutani H, Kishimoto T. Molecular cloning and structure of a pre-B-cell growth-stimulating factor. *Proc Natl Acad Sci U S A*. 1994;91:2305–2309.
2. Bleul CC, Farzan M, Choe H, et al. The lymphocyte chemoattractant SDF-1 is a ligand for LESTR/fusin and blocks HIV-1 entry. *Nature*. 1996;382:829–833.
3. Nagasawa T, Hirota S, Tachibana K, et al. Defects of B-cell lymphopoiesis and bone-marrow myelopoiesis in mice lacking the CXC chemokine PBSF/SDF-1. *Nature*. 1996;382:635–638.
4. Tachibana K, Hirota S, Iizasa H, et al. The chemokine receptor CXCR4 is essential for vascularization of the gastrointestinal tract. *Nature*. 1998; 393:591–594.
5. Zou YR, Kottmann AH, Kuroda M, et al. Function of the chemokine receptor CXCR4 in haematopoiesis and in cerebellar development. *Nature*. 1998;393:595–599.
6. Mohle R, Bautz F, Rafii S, et al. The chemokine receptor CXCR-4 is expressed on CD34$^+$ hematopoietic progenitors and leukemic cells and mediates transendothelial migration induced by stromal cell-derived factor-1. *Blood*. 1998;91:4523–4530.
7. Lataillade JJ, Clay D, Dupuy C, et al. Chemokine SDF-1 enhances circulating CD34(+) cell proliferation in synergy with cytokines: possible role in progenitor survival. *Blood*. 2000;95:756–768.
8. Hattori K, Heissig B, Tashiro K, et al. Plasma elevation of stromal cell-derived factor-1 induces mobilization of mature and immature hematopoietic progenitor and stem cells. *Blood*. 2001;97:3354–3360.
9. Salcedo R, Wasserman K, Young HA, et al. Vascular endothelial growth factor and basic fibroblast growth factor induce expression of CXCR4 on human endothelial cells: in vivo neovascularization induced by stromal-derived factor-1α. *Am J Pathol*. 1999;154:1125–1135.
10. Asahara T, Murohara T, Sullivan A, et al. Isolation of putative progenitor endothelial cells for angiogenesis. *Science*. 1997;275:964–967.
11. Shi Q, Rafii S, Wu MH, et al. Evidence for circulating bone marrow-derived endothelial cells. *Blood*. 1998;92:362–367.
12. Orlic D, Kajstura J, Chimenti S, et al. Bone marrow cells regenerate infarcted myocardium. *Nature*. 2001;410:701–705.
13. Takahashi T, Kalka C, Masuda H, et al. Ischemia- and cytokine-induced mobilization of bone marrow-derived endothelial progenitor cells for neovascularization. *Nat Med*. 1999;5:434–438.
14. Lyden D, Hattori K, Dias S, et al. Impaired recruitment of bone-marrow-derived endothelial and hematopoietic precursor cells blocks tumor angiogenesis and growth. *Nat Med*. 2001;7:1194–1201.
15. Kawamoto A, Gwon HC, Iwaguro H, et al. Therapeutic potential of ex vivo expanded endothelial progenitor cells for myocardial ischemia. *Circulation*. 2001;103:634–637.
16. Kalka C, Masuda H, Takahashi T, et al. Transplantation of ex vivo expanded endothelial progenitor cells for therapeutic neovascularization. *Proc Natl Acad Sci U S A*. 2000;97:3422–3427.
17. Asahara T, Takahashi T, Masuda H, et al. VEGF contributes to postnatal neovascularization by mobilizing bone marrow-derived endothelial progenitor cells. *EMBO J*. 1999;18:3964–3972.
18. McDonald DM, Munn L, Jain RK. Vasculogenic mimicry: how convincing, how novel, and how significant? *Am J Pathol*. 2000;156: 383–388.
19. Moldovan NI, Goldschmidt-Clermont PJ, Parker-Thornburg J, et al. Contribution of monocytes/macrophages to compensatory neovascularization: the drilling of metalloelastase-positive tunnels in ischemic myocardium. *Circ Res*. 2000;87:378–384.
20. Asahara T, Masuda H, Takahashi T, et al. Bone marrow origin of endothelial progenitor cells responsible for postnatal vasculogenesis in physiological and pathological neovascularization. *Circ Res*. 1999;85: 221–228.

Journal of the American College of Cardiology
© 2003 by the American College of Cardiology Foundation
Published by Elsevier Science Inc.

Vol. 41, No. 6, 2003
ISSN 0735-1097/03/$30.00
doi:10.1016/S0735-1097(02)03007-3

Biodegradable Gelatin Hydrogel Potentiates the Angiogenic Effect of Fibroblast Growth Factor 4 Plasmid in Rabbit Hindlimb Ischemia

Hirofumi Kasahara, MD,* Etsuro Tanaka, MD, PHD,†§ Naoto Fukuyama, MD, PHD,†§ Eriko Sato, MD,* Hiromi Sakamoto, PHD,‖ Yasuhiko Tabata, PHD,¶ Kiyoshi Ando, MD, PHD,‡§ Harukazu Iseki, MD, PHD,‡ Yoshiro Shinozaki, BS,† Koji Kimura, MD,* Eriko Kuwabara, MD,* Shirosaku Koide, MD, PHD,* Hiroe Nakazawa, MD, PHD,† Hidezo Mori, MD, PHD#

Isehara, Tokyo, Kyoto, and Suita, Japan

OBJECTIVES We investigated the potentiation of gene therapy using fibroblast growth factor 4 (FGF4)-gene by combining plasmid deoxyribonucleic acid (DNA) with biodegradable gelatin hydrogel (GHG).

BACKGROUND Virus vectors transfer genes efficiently but are biohazardous, whereas naked DNA is safer but less efficient. Deoxyribonucleic acid charges negatively; GHG has a positively charged structure and is biodegradable and implantable; FGF4 has an angiogenic ability.

METHODS The GHG-DNA complex was injected into the hindlimb muscle (63 mice and 55 rabbits). Gene degradation was evaluated by using ^{125}I-labeled GHG-DNA complex in mice. Transfection efficiency was evaluated with reverse-transcription nested polymerase chain reaction and X-Gal histostaining. The therapeutic effects of GHG-FGF4-gene complex (GHG-FGF4) were evaluated in rabbits with hindlimb ischemia.

RESULTS Gelatin hydrogel maintained plasmid in its structure, extending gene degradation temporally until 28 days after intramuscular delivery, and improving transfection efficiency. Four weeks after gene transfer, hindlimb muscle necrosis was ameliorated more markedly in the GHG-FGF4 group than in the naked FGF4-gene and GHG-beta-galactosidase (control) groups ($p < 0.05$, Kruskal-Wallis test). Synchrotron radiation microangiography (spatial resolution, 20 μm) and flow determination with microspheres confirmed significant vascular responsiveness to adenosine administration in the GHG-FGF4 group, but not in the naked FGF4-gene and the control.

CONCLUSIONS The GHG-FGF4 complex promoted angiogenesis and blood flow regulation of the newly developed vessels possibly by extending gene degradation and improving transfection efficiency without the biohazard associated with viral vectors. (J Am Coll Cardiol 2003;41: 1056–62) © 2003 by the American College of Cardiology Foundation

Angiogenic gene therapy using growth factors is widely studied to treat ischemic heart disease and severe limb ischemia (1,2). Of the two major methods of gene transfer, the use of virus vectors is efficient but biohazardous (3,4), while naked deoxyribonucleic acid (DNA) is safer, but less efficient (5). A highly efficient and safe drug delivery system without using a virus vector is needed for gene therapy in humans. We developed a new hydrogel consisting of amino acids, being biodegradable and, therefore, implantable, from gelatin (6). Hydrogel has been used to improve transfection efficiency in a hydrogel-coated balloon catheter (7). However, this hydrogel was not implantable because it consisted of carbohydrate and was not biodegradable. The purpose of the present study is to assess whether biodegradable gelatin hydrogel (GHG) improves the efficacy of gene therapy with the fibroblast growth factor 4 (FGF4)/hst1 gene; FGF4 is a growth factor discovered in human gastric cancer (8) and has a secretion signal domain (9). Its angiogenic ability has been confirmed both in vitro and in vivo (10).

From the Departments of *Cardiovascular Surgery, †Physiology, ‡Internal Medicine, and §Research Center for Genetic Engineering and Cell Transplantation, Tokai University School of Medicine, Isehara, Japan; ‖Genetics Division, National Cancer Center Research Institute, Tokyo, Japan; ¶Research Center for Biomedical Engineering, Kyoto University, Kyoto, Japan; #Department of Cardiac Physiology, National Cardiovascular Center Research Institute, Suita, Japan. Supported by Grants-in-Aid for Scientific Research (13470154, 13470381, 13877114, 14657460, 14657461) from the MECSST; New Energy and Industrial Technology Development Organization; The Science Frontier Program of MESSC; The Research Grants for Cardiovascular Disease (H13C-1) and for Cancer Research (9-3, 10Shi-1) from the MHLW; HLSRG-H14nano001&genom005; the Promotion of Fundamental Studies in Health Science of the Organization for Pharmaceutical Safety and Research of Japan.

Manuscript received December 30, 2001; revised manuscript received July 2, 2002, accepted November 5, 2002.

METHODS

Experimental animals. All animal experiments were performed in accordance under the Guidelines of Tokai University School of Medicine on Animal Use, which conform to the National Institute of Health (NIH) Guide for the Care and Use of Laboratory Animals, DHEW publication No. (NIH) 86-23, revised 1985, Offices of Science and Health Reports, DRR/NIH, Bethesda, Maryland. Fifty-five Japanese white rabbits weighting 2.45 to 2.85 kg (Nihon Nosan Co., Tokyo, Japan) of both genders were used. The animals were anesthetized by intravenous injection of sodium pentobarbital (40 mg/kg), and hindlimb ischemia was created by the method of Takeshita et al. (11). Sixty-three

Abbreviations and Acronyms

ANOVA	= analysis of variance
cDNA	= complementary deoxyribonucleic acid
DNA	= deoxyribonucleic acid
FGF4	= fibroblast growth factor 4
GHG	= gelatin hydrogel
lacZ	= beta-galactosidase
NIH	= National Institute of Health
PBS	= phosphate-buffered saline
pI	= isoelectric point
RNA	= ribonucleic acid
RT-nested PCR	= reverse transcription-nested polymerase chain reaction

mice (male ddY mice, six to seven weeks old, Shizuoka Animal Center, Shizuoka, Japan) were also used.

Preparation of GHG-DNA complex. DNA encoding FGF4, beta-galactosidase (lacZ) with the cytomegalovirus enhancer-chicken β-actin hybrid promoter comprising a cytomegalovirus enhancer, and chicken beta-actin promoter were constructed (12); GHG was prepared from bovine bone (6). The GHG used in this study was characterized by a spheroid shape with a diameter of approximately 200 μm, water content of 95%, and an isoelectric point (pI) of 11 after swelling in water, without special statement.

The efficiency of incorporation of DNA into positively and negatively charged GHG was evaluated. Dried GHG (4 mg, pI 11 or 5) was added to lacZ DNA solution (500 μg/100 μl in phosphate-buffered saline [PBS], pH 7.4), mixed with a vortex mixer for 5 s, and allowed to stand at 37°C; the solution immediately settled. The absorbance (260 nm) of the supernatant was measured. In a sham control experiment, GHG was added to pure PBS solution. Positively charged GHG (pI 11) was immediately impregnated with naked DNA, and was stable at pH 7.4 for at least 120 h, whereas the negatively charged one (pI 5) was not.

Experimental protocols. PROTOCOL 1: DNA DEGRADATION AND THE IMPROVEMENT OF TRANSFECTION EFFICIENCY BY GHG. To examine the temporal extension of gene degradation by GHG, the decay sequence of ^{125}I-labeled DNA impregnated into unlabeled GHG, ^{125}I-labeled GHG, and ^{125}I-labeled DNA solution was compared (63 mice). Plasmid DNA and GHG were radioiodinated with ^{125}I, with TlCl3 and Bolton and Hunter reagent (Amersham Pharmacia Biotech Ltd., Buckinghamshire, United Kingdom) (13), respectively. To impregnate GHG with DNA, dried GHG (2 mg) was added to 100 μl of naked lacZ solution (50 μg/100 μl in PBS), mixed for 5 s, and allowed to stand at 37°C for 2 h. Each complex was injected into the hindlimb muscle. On days 1, 3, 5, 7, 14, 21, or 28, the muscle was collected, and radioactivity was measured with a gamma counter (ARC-301B, Aloka Co., Ltd., Tokyo, Japan) in three mice each.

The following experiment was performed in 16 rabbits to assess spatial potentiation of gene expression by GHG. Intramuscular gene transfer was performed 10 days after modeling hindlimb ischemia. The DNA solution (FGF4-gene or lacZ 500 μg/100 μl PBS) mixed with GHG (4 mg; GHG-FGF4 complex, n = 2; GHG-lacZ complex, n = 2) and the original FGF4-gene solution (naked FGF4-gene, n = 2) were diluted with 0.4 ml saline and slowly injected through a 23-gauge needle at a single point in the adductor muscle marked with a 4-0 nylon suture. Tissue samples from the transfected left adductor muscle (the injection site and the adjacent region 10 mm apart from the injection site), the right adductor muscle, stomach, liver, spleen, testes, kidneys, heart, lungs, and brain were retrieved and immediately frozen in liquid nitrogen on day 17; FGF4-gene expression was evaluated by reverse transcription-nested polymerase chain reaction (RT-nested PCR). In the remaining 10 rabbits, gene expression was evaluated with lacZ gene; GHG-lacZ complex (n = 5) and naked lacZ solution (n = 5) were injected at a single point in the adductor muscle in the same way as the GHG-FGF4 injection on day 10. On day 17, a muscle sample at the injection site was dissected out, and expression of lacZ was determined by X-Gal histostaining (14).

PROTOCOL 2: SALVAGE OF HINDLIMB ISCHEMIA WITH GHG-PLASMID COMPLEX ENCODING FGF4. The angiogenic effect of three sets of GHG-DNA complexes were compared in 39 rabbits with hindlimb ischemia: 1) GHG impregnated with lacZ plasmid (GHG-lacZ: control); 2) naked FGF4-plasmid (naked FGF4-gene); and 3) GHG impregnated with FGF4 plasmid (GHG-FGF4). The amount of plasmid was 500 μg (1.0 ml) and that of GHG was 4 mg. On day 10 of ischemia, the gene complex was injected at five points 20 mm apart in the adductor muscle with a 23-gauge needle.

In 18 rabbits, on days 10 and 38 of ischemia, calf systolic blood pressure was measured by the Doppler flow signal from the posterior tibial artery (ES-100V2, Hayashi Denki Co., Kawasaki, Japan) with a 25-mm wide cuff. The calf blood pressure ratio of each rabbit was defined as the ratio of the systolic pressure of the ischemic limb to that of the normal limb. Regional blood flow was measured by the microsphere method (15) at baseline on days 0 and 38. On day 38, adenosine (100 μg/kg/min) was administered 30 min after baseline flow measurement (vasodilatory condition). A 4F catheter was introduced into the ascending aorta via the common carotid artery for microsphere injection and adenosine administration. Microspheres (15-μm diameter, 3 × 106) labeled with one of four sets of stable heavy elements (In, I, Ba, or Ce, Sekisui Plastic, Osaka, Japan) (15) were suspended in 0.05% sodium dodecyl sulfate at a concentration of 5 × 106/ml and injected into the ascending aorta. After killing the animals, the adductor, semimembranous, and gastrocnemius muscles were dissected out and weighed. The X-ray fluorescence of the labeled microspheres was measured in 4 to 8 g of the dissected muscles to calculate the regional blood flow (15) and expressed as the ratio of flow in the ischemic limb to flow in the normal limb.

JACC Vol. 41, No. 6, 2003
March 19, 2003:1056–62

Table 1. Morphologic Evaluation of Gene Therapy

Muscle Necrosis (Area)	GHG-lacZ	Naked FGF4	GHG-FGF4*†
Grade 0 (0 cm^2)	0	0	0
Grade 1 (<1 cm^2)	0	0	50% (3/6)
Grade 2 (<3 cm^2)	17% (1/6)	33% (2/6)	50% (3/6)
Grade 3 (<5 cm^2)	0	67% (4/6)	0
Grade 4 (<10 cm^2)	50% (3/6)	0	0
Grade 5 (>10 cm^2)	33% (2/6)	0	0
Muscle weight ratio (%)	48 ± 67 (6)	62 ± 14 (6)	79 ± 11* (6)

Morphologic indexes in 18 gene-transferred rabbits on day 38. The ischemic limb was macroscopically evaluated by using graded morphological scales for muscle necrosis area (the adductor, semimembranous, medial large, and gastrocnemius muscles) (grade 0 to 5); GHG-FGF4 group had significantly less muscle necrosis compared with naked FGF4 and GHG-lacZ groups. Muscle weight ratio was significantly different between GHG-FGF4 and GHG-lacZ groups. $p < 0.05$ vs. *GHG-lacZ, †naked FGF4 (Kruskal-Wallis test, analysis of variance).

FGF4 = fibroblast growth factor 4; GHG = gelatin hydrogel; lacZ = β-galactosidase.

Sufficient mixing of microspheres injected into the aorta (not into the left atrium) was confirmed by a preliminary study in which two different sets of microspheres were simultaneously injected into the aorta. The liner regression analysis on the two different sets of flows yielded an almost identical regression line ($y = 1.011x - 0.003$, $r = 0.98$, $Sy \cdot x = 0.032$). The remaining muscle tissue was used for histological analysis. An investigator blinded to the treatment macroscopically evaluated the ischemic limb on graded morphological scales for area of muscle necrosis (the adductor, semimembranous, medial large, and gastrocnemius muscles; grade 0 to 5; Table 1).

Synchrotron radiation microangiography characterized by high-resolution and high-sensitivity (16) was performed in 21 rabbits as previously described (15,17,18). The system is capable of separating adjacent lead lines only 20 μm apart on the resolution bar chart with 640× higher sensitivity than charge-coupled device camera system. This system allows detection and functional analysis of small vessels with a diameter of 200 to 500 μm in situ (15,17,18). Contrast material containing 37% nonionic iodine (Iopamidol, Nihon Schering Co., Tokyo, Japan) was injected via a 4F catheter placed immediately above the aortic bifurcation under baseline condition and during adenosine administration (100 μg/kg/min) (vasodilatory condition) via the same catheter. Vessel density in the midzone collateral was evaluated as an angiographic score (11,15,18).

Plasmid. Complementary deoxyribonucleic acid (cDNA) of human hst1/FGF4 (19), or bacterial β-galactosidase was inserted into the expression vector pRC/CMV (Invitrogen Corp., Carlsbad, California) and designated as pRC/CMV-HST1-10 (human stomach tumor) and pRC/CMV-lacZ, respectively. Preparation and purification of the plasmid from cultures of pRC/CMV-HST1-10-, or pRC/CMV-lacZ-transformed *Escherichia coli* were performed by centrifugation to equilibrium in cesium chloride-ethidium bromide gradients.

RT-nested PCR. Ribonucleic acid (RNA) was extracted from tissues with ISOGEN (Nippon Gene, Tokyo, Japan). The extracted RNA was treated with DNase twice to eliminate DNA contamination. In each set of experiments, 0.5 μg of total RNA was denatured at 70°C for 5 min, and reverse transcription was carried out at 37°C for 60 min; RT-nested PCR was carried out in a thermal cycler (GeneAmp PCR System 9600, Perkin Elmer, Wellesley, Massachusetts) with primers designed to selectively amplify the FGF4 cDNA. The external primers EcoHST1f3 (forward primer: GGA ATT CAC TGA CCG CCT GAC CGA CGC ACG GCC CTC G) and SalHST1r2 (reverse primer: GCG TCG ACC CCG AGG CTG AGG CAA GGG TCC TCT) were used for the first round (generating a 704-base pair [bp] fragment). The second round of the amplification (nested PCR) was performed with two internal primers HST1LGC1 (forward primer: AGC TCT CGC CCG TGG AGC GG) and HST1AA-r (reverse primer: CTC TGG AGG GTC ACA GCC TG) (generating a 282-bp fragment). The PCR reactions were performed as follows. The thermal cycle conditions for the first round were 30 cycles (95°C for 1 min, 59°C for 1 min, 72°C for 1 min), and for the second round were 25 cycles (94°C for 1 min, 72°C for 2 min), followed by incubation at 72°C for 10 min, respectively. Amplification products were detected after electrophoresis on 3.5% agarose gels by staining with ethidium bromide. A primer set of beta-actin (generating a 506-bp fragment) was used as a positive control for RT-PCR analysis.

Statistical analysis. Data are presented as mean values ± SD. Differences were assessed by using the paired *t* test, Kruskal-Wallis test, or analysis of variance (ANOVA) for factorial or repeated measures with the Scheffé F test when applicable. A value of $p < 0.05$ was considered statistically significant.

RESULTS

Protocol 1: DNA degradation and the improvement of transfection efficiency by GHG. The radioactivity of radiolabeled DNA impregnated into GHG in the limb muscle remained above the detection limit for four weeks (solid line in Fig. 1). The radiolabeled DNA impregnated into GHG had decay sequences almost identical to those of the radiolabeled GHG (dotted line in Fig. 1). By contrast, the radioactivity of naked DNA (dashed line in Fig. 1) decreased to <10% of the baseline within a day.

Gelatin hydrogel improved transfection efficiency in vivo; RT nested-PCR analyses revealed FGF4 expression at all injection sites in the left adductor muscle in the FGF4-gene-treated animals ($n = 4$), as shown in lanes 1 (naked FGF4-gene) and 4 (GHG-FGF4) in Figure 2; FGF4 expression was also detected in the adjacent region 10 mm apart from the injection site in the left adductor muscle in the GHG-FGF4-treated animals (lane 5), but not in the naked FGF4-gene-treated animals (lane 2). No expression was detected in any animal at remote sites, such as the right adductor muscle (lanes 3 and 6), stomach, liver, spleen,

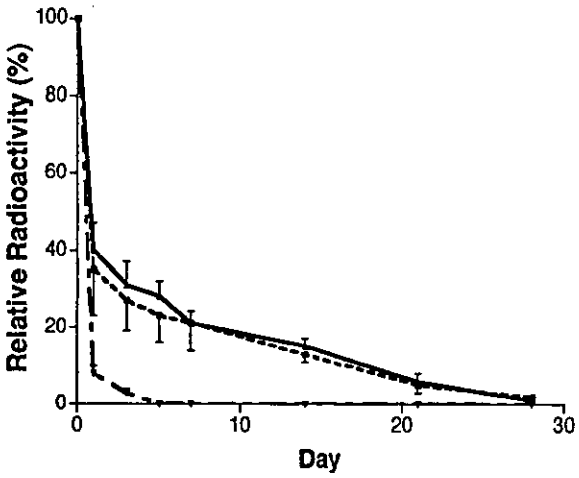

Figure 1. Decay sequences of radiolabeled deoxyribonucleic acid (DNA), gelatin hydrogel (GHG), and DNA combined with GHG in the hindlimb muscles of mice. Unlabeled GHG impregnated with ^{125}I-labeled DNA **(solid line)**, ^{125}I-labeled GHG **(dashed line)**, and ^{125}I-labeled DNA solution **(dotted line)** were injected into the hindlimb muscles.

testes, kidneys, heart, lungs, or brain (data not shown); lacZ-treated animals showed no FGF4 expression at any sites (lanes 7 and 8). Beta-actin expression was detected in all samples (lower panel), but neither beta-actin nor FGF4 expression was detected in any control samples that were not treated with reverse transcriptase; lacZ expression of naked DNA (500 μg) was localized to the injection site (Fig. 3A), whereas GHG-DNA complex (DNA amount 500 μg) showed a spatially expanded expression on day 17 (Fig. 3B). The degree of gene expression in myocytes was also augmented by GHG.

Protocol 2: salvage of hindlimb ischemia with GHG-plasmid complex encoding FGF4. Functional evaluation of ischemic hindlimbs showed amelioration of the ischemia

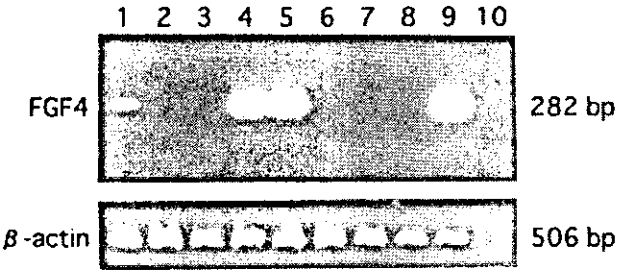

Figure 2. Representative transgene expression demonstrated by reverse-transcription nested polymerase chain reaction (RT-nested PCR). The left adductor muscle of the rabbits was injected with naked fibroblast growth factor 4 (FGF4) gene **(lanes 1 to 3)**, gelatin hydrogel (GHG)-FGF4 **(lanes 4 to 6)**, or GHG-lacZ **(lanes 7 and 8)**. Each sample was obtained from the injection site **(lanes 1, 4, and 7)** and the adjacent region 10 mm apart from the injection site **(lanes 2, 5 and 8)** in the left adductor muscle, and from the contralateral adductor muscle **(lanes 3 and 6)**. The RT-nested PCR products from ribonucleic acid of each sample were analyzed on agarose gel; FGF4 expressed Cc1/l6 cells as a positive control **(lane 9)** and no deoxyribonucleic acid (DNA) template as a negative control **(lane 10)**. A housekeeping beta-actin gene was amplified as a complementary DNA loading control.

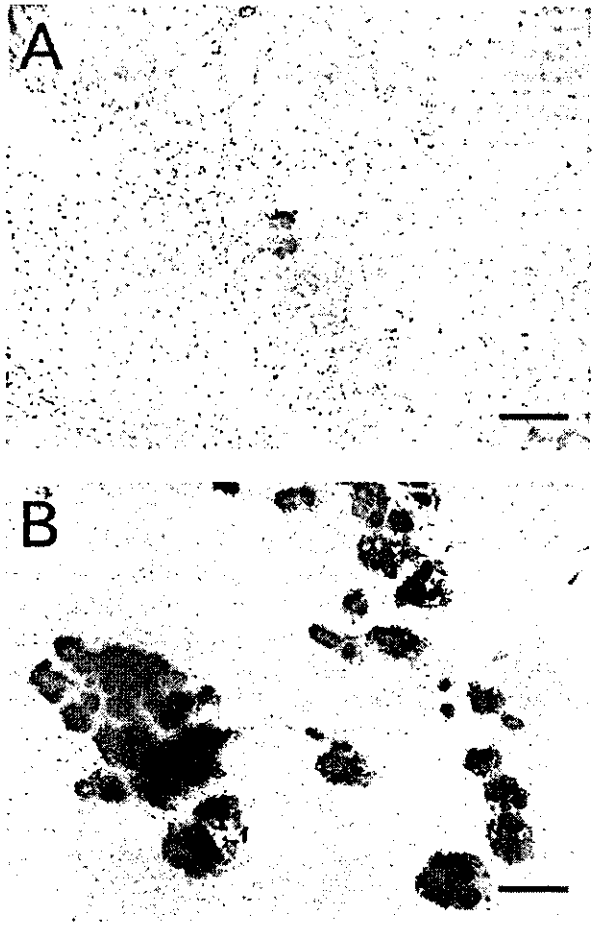

Figure 3. Representative gene expression of lacZ in the ischemic adductor muscle in rabbits on day 17. Naked deoxyribonucleic acid (DNA) **(A)** or gelatin hydrogel-DNA complex **(B)** was injected into the adductor muscle 10 days after the ischemic insult. X-Gal stain; original magnification ×20; **bar** = 200 μm.

by the FGF4-gene and potentiation of the amelioration when GHG was used as a delivery device. The augmentation of regional blood flow with GHG was more evident under vasodilatory conditions than at the baseline.

Regional blood flow analysis and angiographic analysis further confirmed the background mechanism for amelioration of hindlimb ischemia by GHG-FGF4 (Table 2). On day 38, blood flow during adenosine administration (vasodilatory condition) in the GHG-FGF4 group (105 ± 13% in terms of ischemic/normal flow ratio) was significantly higher than in either the naked FGF4-gene group (68 ± 18%, $p < 0.05$) or the GHG-lacZ group (50 ± 12%, $p < 0.05$, ANOVA). The differences between the naked FGF4-gene and GHG-lacZ groups were not significant (ANOVA). The adenosine-dependent flow-augmentation (responsiveness to vasodilatory stimulation; comparison between adenosine and baseline values on day 38) was noted only in the GHG-FGF4 group (from 79 ± 16% to 105 ± 13%, $p < 0.05$, ANOVA), and not in the other two groups. A similar tendency was noted in flow under baseline conditions on day 38 in all three groups; however, the

JACC Vol. 41, No. 6, 2003
March 19, 2003:1056–62

Table 2. Functional Evaluation of Gene Therapy

	GHG-lacZ	Naked FGF4	GHG-FGF4
Blood flow ratio (%) (ischemic/normal)			
Day 0 (BL)	33 ± 8 (6)	36 ± 11 (6)	37 ± 10 (6)
Day 38 (BL)	47 ± 12‡ (6)	58 ± 16‡ (6)	79 ± 16*‡ (6)
Day 38 (Ad)	50 ± 12‡ (6)	68 ± 18‡ (6)	105 ± 13*†‡§ (6)
Angiographic score			
Day 38 (BL)	0.37 ± 0.12 (7)	0.39 ± 0.13 (7)	0.42 ± 0.11 (7)
Day 38 (Ad)	0.36 ± 0.10 (7)	0.41 ± 0.13 (7)	0.56 ± 0.15*†§ (7)
Blood pressure (%) (ischemic/normal)			
Day 10	31 ± 8 (6)	33 ± 5 (6)	26 ± 7 (6)
Day 38	56 ± 4 (6)	63 ± 6 (6)	70 ± 11* (6)

Angiographic score was calculated on the synchrotron radiation microangiogram. $p < 0.05$ vs. *GHG-lacZ, †naked FGF4, ‡day 0 (BL), and §day 38 (BL) (analysis of variance).

Ad = during adenosine administration; BL = under baseline condition; FGF4 = fibroblast growth factor 4; GHG = gelatin hydrogel; lacZ = β-galactosidase.

differences in baseline flow among the three groups were less marked than during adenosine administration.

Synchrotron radiation microangiography revealed microvessel responsiveness to the vasodilatory stimulation in the GHG-FGF4-treated rabbits (Figs. 4C and 4D), whereas vascular density was somewhat decreased by adenosine treatment in some of the GHG-lacZ-treated rabbits (Figs. 4A and 4B). Angiographic score analysis yielded quantitative evidence (Table 2). The angiographic score during adenosine administration (vasodilatory condition) was significantly higher in the GHG-FGF4 group (0.56 ± 0.15) than in either the naked FGF4-gene group (0.41 ± 0.13, $p < 0.05$) or the GHG-lacZ group (0.36 ± 0.10, $p < 0.05$, ANOVA). By contrast, under baseline conditions, the angiographic scores of the three groups were not significantly different.

On day 38, the GHG-FGF4 group had the highest calf-blood pressure ratio (70 ± 11%), and it was lower in the naked FGF4-gene group (63 ± 6%), and even lower in the GHG-lacZ group (56 ± 4%, $p < 0.05$ vs. the GHG-lacZ group, ANOVA, Table 2). On day 10 (the time of gene transfer), the degrees of decrease in the three groups were not significantly different (26% to 33% in the mean).

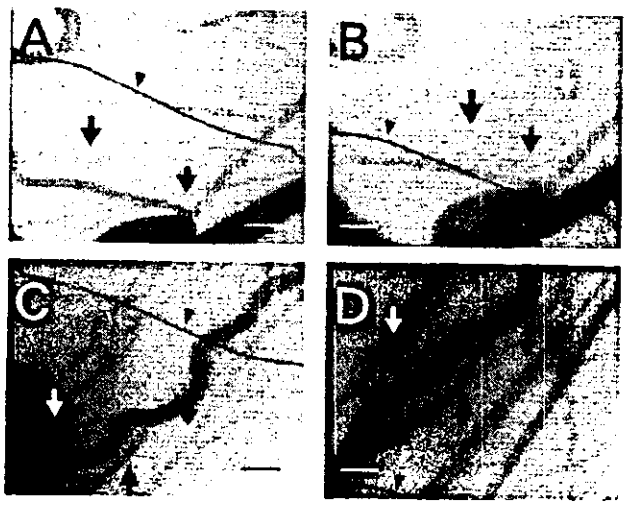

Figure 4. Representative synchrotron radiation microangiograms of the hindlimb ischemia in the rabbits. Synchrotron radiation microangiograms were taken under baseline conditions **(A and C)** and after repeated adenosine administration **(B and D)** on day 38. **(A and B)** Gelatin hydrogel (GHG)-lacZ-treated rabbit; **(C and D)** GHG-fibroblast growth factor 4-treated rabbit. **Arrows** indicate the same point in the vessels. **Arrowheads** reference copper wires with a diameter of 130 μm; **bar** = 1 mm.

Tissue damage was least in the GHG-FGF4-treated rabbits (Table 1). Limb muscle necrosis was <3 cm^2 and grade 1 or 2 in all of the animals in the GHG-FGF4 group, and significantly less than in the other two groups ($p < 0.05$, Kruskal-Wallis test). A similar difference was noted in the degrees of toe necrosis (data not shown). The muscle weight ratio (ischemic/normal) on day 38 was highest in the GHG-FGF4 group (79 ± 11%), lower in the naked FGF4-gene group (62 ± 14%), and even lower in the GHG-lacZ group (48 ± 67%), and the difference between the GHG-FGF4 group and GHG-lacZ group was significant ($p < 0.05$, ANOVA). The muscle weight ratio values (a morphological index) positively correlated with vascular responsiveness to adenosine (adenosine/baseline blood flow ratio [%]; a functional index) ($r = 0.50$, $n = 18$, $Sy \cdot x = 0.15$, $Sy \cdot x/y = 0.23$, $p = 0.045$). Thus, the blood flow, microangiographic, and morphologic analyses demonstrated a greater ameliorative effect of the GHG-FGF4 complex compared with the naked FGF4-gene (Tables 1 and 2).

Minimal inflammatory infiltrates, such as neutrophil and lymphoplasmacytic cell infiltrates, were noted at the injection site, but histological analysis showed that the infiltrates were localized. There was no evidence of fibrous proliferation or tumor formation in the transfected muscles or in other organs (right adductor muscle, stomach, liver, spleen, testes, kidneys, heart, lungs, and brain) in any of the groups.

DISCUSSION

We demonstrated that GHG potentiated the angiogenic effect of the FGF4-gene (protocol 2) by prolonging DNA degradation and improving transfection efficiency (protocol 1). Thus, GHG might facilitate the gene therapy of intractable circulatory disorders with genes for angiogenic growth factors.

Gelatin hydrogel augmented the effect of the FGF4-gene

therapy by improving gene biodegradation and transfection efficiency. We demonstrated that GHG rapidly absorbed plasmid DNA and did not release it in vitro (see Methods section). In the radioiodine experiment, the radioactivity of naked DNA was reduced to less than 10% of the baseline within a day, whereas the radioactivity of DNA impregnated into GHG remained for four weeks (Fig. 1). In the experiment using the rabbit hindlimb ischemia model, the PCR analysis suggested that GHG expanded the gene transfer spatially (lanes 2 and 5 in Fig. 2). The maker gene experiment (protocol 1) confirmed that the use of GHG augmented both the number of transfected myocytes and the degree of gene expression in these cells, and also supported the spatially expanded gene expression (Fig. 3). The superiority of the therapeutic effects of the GHG-FGF4-gene complex on hindlimb ischemia compared with naked FGF4-gene treatment was confirmed in the rabbit experiments in protocol 2 (Fig. 4, Tables 1 and 2); GHG-FGF4-treated rabbits were characterized by less severe tissue damage in the ischemic limb (Table 2) and more marked vascular responsiveness to adenosine than either the naked FGF4-treated or GHG-lacZ-treated rabbits (Fig. 4, Table 2, Protocol 2 in the Results section). Under the baseline conditions, blood flow in normal muscle tissue is set at a relatively low level in preparation for an abrupt increase in flow demand (approximately 5× and 30× in the heart and in the skeletal muscle, respectively) during exercise, etc. (responsiveness to the vasodilatory stimulation). In other words, normal muscle tissue has a sufficient flow reserve (20,21), and, thus, the presence or absence of vascular responsiveness to adenosine administration can be used as an index of fundamental vascular function in angiogenic vascular segments. The demonstration of a positive correlation between flow responsiveness to adenosine and the muscle weight ratio further supports our hypothesis. Baseline flow may reflect the total number of angiogenic vessels, if it does not respond to vasodilatory stimulation. However, if the vasodilatory mechanism is present, baseline flow alone does not necessarily reflect the quality and/or quantity of angiogenic vascular segments. The amelioration of the ischemic tissue in the GHG-FGF4 group may be related to an adequate flow reserve (20,21) of so-called "well-tempered angiogenic vessels" (22).

Consequently, GHG offers several advantages as a new gene delivery system: 1) it has a positively charged structure, so it holds negatively charged nucleic acids, proteins, and drugs within its structure; 2) GHG is biodegradable and implantable; the biodegradable nature is from the gelatin itself but not from the hydrogel state. The substance bound to the GHG is gradually released as the gelatin degrades in situ. The degradation period can be adjusted to two to four weeks by varying the water content. Thus, the prolonged release of the DNA held in GHG was presumably responsible for the augmentation of gene therapy. The use of hydrogel-coated balloon-angioplasty-catheter has been reported (7). However, this gel is much different from our hydrogel. The present GHG consists of amino acids and is biodegradable and implantable, whereas their hydrogel consists of carbohydrate and is not biodegradable nor implantable. 3) The isoelectric point and the shape of the GHG can be modified. Negatively charged GHG holds positively charged substances such as basic-FGF protein (6,23), and disk-shaped GHG has been found to be effective for reconstruction of bone defects (23); 4) GHG is less biohazardous than adenovirus vectors. Gelatin is already used in the clinical field, and its safety is established. Thus, the use of GHG with naked DNA improves its transfection efficiency without causing serious cytotoxicity or biohazards, which are inconvenient side effects of virus vectors (24). Therefore, the nonvirus vector GHG is useful for various gene therapies including the treatment of cardiovascular disorders.

Acknowledgments

The authors wish to thank Chiharu Tada, Akiko Hori, Sachie Ueno, and Takayuki Hasegawa for their technical work.

Reprint requests and correspondence: Dr. Hidezo Mori, Department of Cardiac Physiology, National Cardiovascular Center Research Institute, 5-7-1 Fujishirodai, Suita 565-8565, Japan. E-mail: hidemori@ri.ncvc.go.jp.

REFERENCES

1. Asahara T, Bauters C, Zheng LP, et al. Synergistic effect of vascular endothelial growth factor and basic fibroblast growth factor on angiogenesis in vivo. Circulation 1995;92:417–27.
2. Aoki M, Morishita R, Taniyama Y, et al. Angiogenesis induced by hepatocyte growth factor in non-infarcted myocardium and infarcted myocardium: up-regulation of essential transcription factor for angiogenesis. Gene Ther 2000;7:417–27.
3. Yang Y, Trinchieri G, Wilson JM. Recombinant IL-12 prevents formation of blocking IgA antibodies to recombinant adenovirus and allows repeated gene therapy to mouse lung. Nat Med 1995;1:890–3.
4. Zabner J, Ramsey BW, Meeker DP, et al. Repeat administration of an adenovirus vector encoding cystic fibrosis transmembrane conductance regulator to the nasal epithelium of patients with cystic fibrosis. J Clin Invest 1996;97:1504–11.
5. Takeshita S, Isshiki T, Sato T. Increased expression of direct gene transfer into skeletal muscles observed after acute ischemic injury in rats. Lab Invest 1996;74:1061–5.
6. Tabata Y, Hijikata S, Muniruzzaman M, Ikada Y. Neovascularization effect of biodegradable gelatin microspheres incorporating basic fibroblast growth factor. J Biomater Sci Polym Ed 1999;10:79–94.
7. Isner JM, Pieczek A, Schainfeld R, et al. Clinical evidence of angiogenesis after arterial gene transfer of phVEGF165 in patients with ischaemic limb. Lancet 1996;348:370–4.
8. Sakamoto H, Mori M, Taira M, et al. Transforming gene from human stomach cancers and a noncancerous portion of stomach mucosa. Proc Natl Acad Sci USA 1986;83:3997–4001.
9. Fuller PF, Peters G, Dickson C. Cell transformation by kFGF requires secretion but not glycosylation. J Cell Biol 1991;115:547–55.
10. Yoshida T, Ishimaru K, Sakamoto H, et al. Angiogenic activity of the recombinant hst-1 protein. Cancer Lett 1994;83:261–8.
11. Takeshita S, Zheng LP, Brogi E, et al. Therapeutic angiogenesis: a single intra-arterial bolus of vascular endothelial growth factor augments revascularization in a rabbit ischemic hind limb model. J Clin Invest 1994;93:662–70.
12. Miyazaki J, Takaki S, Araki K, et al. Expression vector system based on the chicken beta-actin promoter directs efficient production of interleukin-5. Gene 1989;79:269–77.

13. Bolton AE, Hunter WM. The labelling of proteins to high specific radioactivities by conjugation to a ^{125}I-containing acylating agent. Biochem J 1973;133:529–39.
14. Ueno H, Li JJ, Tomita H, et al. Quantitative analysis of repeat adenovirus-mediated gene transfer into injured canine femoral arteries. Arterioscler Thromb Vasc Biol 1995;15:2246–53.
15. Tanaka E, Hattan N, Ando K, et al. Amelioration of microvascular myocardial ischemia by gene transfer of vascular endothelial growth factor in rabbits. J Thorac Cardiovasc Surg 2000;120:720–8.
16. Tanioka K, Yamazaki J, Shidara K, et al. Avalanche-mode amorphous selenium photoconductive target for camera tube. Adv Electronics Electron Phys 1988;74:379–87.
17. Mori H, Hyodo K, Tanaka E, et al. Small-vessel radiography in situ with monochromatic synchrotron radiation. Radiology 1996;201:173–7.
18. Takeshita S, Isshiki T, Ochiai M, et al. Endothelium-dependent relaxation of collateral microvessels after intramuscular gene transfer of vascular endothelial growth factor in a rat model of hindlimb ischemia. Circulation 1998;98:1261–3.
19. Taira M, Yoshida T, Miyagawa K, Sakamoto H, Terada M, Sugimura T. cDNA sequence of human transforming gene hst and identification of the coding sequence required for transforming activity. Proc Natl Acad Sci USA 1987;84:2980–4.
20. Austin RJ, Aldea GS, Coggins DL, Flynn AE, Hoffman JI. Profound spatial heterogeneity of coronary reserve: discordance between patterns of resting and maximal myocardial blood flow. Circ Res 1990;67:319–31.
21. Coggins DL, Flynn AE, Austin RJ, et al. Nonuniform loss of regional flow reserve during myocardial ischemia in dogs. Circ Res 1990;67:253–64.
22. Blau H, Banfi A. The well-tempered vessel. Nat Med 2001;7:532–4.
23. Yamada K, Tabata Y, Yamamoto K, et al. Potential efficacy of basic fibroblast growth factor incorporated in biodegradable hydrogels for skull bone regeneration. J Neurosurg 1997;86:871–5.
24. Marshall E. Gene therapy death prompts review of adenovirus vector. Science 1999;286:2244–5.

Hybrid Cell–Gene Therapy for Pulmonary Hypertension Based on Phagocytosing Action of Endothelial Progenitor Cells

Noritoshi Nagaya, MD; Kenji Kangawa, PhD; Munetake Kanda, MD; Masaaki Uematsu, MD; Takeshi Horio, MD; Naoto Fukuyama, MD; Jun Hino, PhD; Mariko Harada-Shiba, MD; Hiroyuki Okumura, MD; Yasuhiko Tabata, PhD; Naoki Mochizuki, MD; Yoshihide Chiba, MD; Keisuke Nishioka, MD; Kunio Miyatake, MD; Takayuki Asahara, MD; Hiroshi Hara, MD; Hidezo Mori, MD

Background—Circulating endothelial progenitor cells (EPCs) migrate to injured vascular endothelium and differentiate into mature endothelial cells. We investigated whether transplantation of vasodilator gene-transduced EPCs ameliorates monocrotaline (MCT)-induced pulmonary hypertension in rats.

Methods and Results—We obtained EPCs from cultured human umbilical cord blood mononuclear cells and constructed plasmid DNA of adrenomedullin (AM), a potent vasodilator peptide. We used cationic gelatin to produce ionically linked DNA-gelatin complexes. Interestingly, EPCs phagocytosed plasmid DNA-gelatin complexes, which allowed nonviral, highly efficient gene transfer into EPCs. Intravenously administered EPCs were incorporated into the pulmonary vasculature of immunodeficient nude rats given MCT. Transplantation of EPCs alone modestly attenuated MCT-induced pulmonary hypertension (16% decrease in pulmonary vascular resistance). Furthermore, transplantation of AM DNA-transduced EPCs markedly ameliorated pulmonary hypertension in MCT rats (39% decrease in pulmonary vascular resistance). MCT rats transplanted with AM-expressing EPCs had a significantly higher survival rate than those given culture medium or EPCs alone.

Conclusions—Umbilical cord blood–derived EPCs had a phagocytosing action that allowed nonviral, highly efficient gene transfer into EPCs. Transplantation of AM gene-transduced EPCs caused significantly greater improvement in pulmonary hypertension in MCT rats than transplantation of EPCs alone. Thus, a novel hybrid cell–gene therapy based on the phagocytosing action of EPCs may be a new therapeutic strategy for the treatment of pulmonary hypertension. **(*Circulation*. 2003;108:889-895.)**

Key Words: pulmonary heart disease ■ natriuretic peptides ■ gene therapy ■ endothelium

The pulmonary endothelium plays an important role in the regulation of pulmonary vascular tone through the release of vasoactive substances such as nitric oxide, prostacyclin, and adrenomedullin (AM).[1] Dysfunction of the endothelium may play a role in the pathogenesis of pulmonary hypertension, including primary pulmonary hypertension.[2] Thus, pulmonary endothelial cells may be a therapeutic target for the treatment of pulmonary hypertension. Recently, endothelial progenitor cells (EPCs) have been discovered in adult peripheral blood.[3] EPCs are mobilized from bone marrow into the peripheral blood in response to tissue ischemia or traumatic injury, migrate to sites of injured endothelium, and differentiate into mature endothelial cells in situ.[4–6] These findings raise the possibility that transplanted EPCs may serve not only as a tissue-engineering tool to reconstruct the pulmonary vasculature but also as a vehicle for gene delivery to injured pulmonary endothelium.

We prepared biodegradable gelatin that could hold negatively charged protein or plasmid DNA in its positively charged lattice structure.[7,8] We have shown that the gelatin is promptly phagocytosed and then gradually degraded by phagocytes, including macrophages.[9] However, whether EPCs phagocytose ionically linked plasmid DNA-gelatin complexes remains unknown. If this is the case, the phago-

Received December 3, 2002; revision received April 17, 2003; accepted April 18, 2003.

From the Departments of Internal Medicine (N.N., T.H., K.M.) and Perinatology (Y.C.), National Cardiovascular Center, Osaka, Japan; Departments of Biochemistry (K.K., J.H., M.H.-S., H.O.), Cardiac Physiology (M.K., H.M.), and Structural Analysis (N.M.), National Cardiovascular Center Research Institute, Osaka, Japan; Cardiovascular Division (M.U.), Kansai Rosai Hospital, Hyogo, Japan; Department of Physiology (N.F.), Tokai University School of Medicine, Kanagawa, Japan; Department of Biomaterials (Y.T.), Field of Tissue Engineering, Institute for Frontier Medical Sciences, Kyoto University, Kyoto, Japan; Department of Transfusion Medicine (K.N., H.H.), Hyogo College of Medicine, Hyogo, Japan; and Department of Regenerative Medicine (T.A.), Institute of Biomedical Research and Innovation, Kobe, Japan.

Reprint requests to Noritoshi Nagaya, MD, or Hidezo Mori, MD, Department of Internal Medicine, National Cardiovascular Center, 5-7-1 Fujishirodai, Suita, Osaka 565-8565, Japan. E-mail nagayann@hsp.ncvc.go.jp or hidemori@ri.ncvc.go.jp

© 2003 American Heart Association, Inc.

Circulation is available at http://www.circulationaha.org

DOI: 10.1161/01.CIR.0000079161.56080.22

cytic activity of EPCs would allow nonviral gene transfer into EPCs. Here we provide rationale of a novel hybrid cell–gene therapy for pulmonary hypertension.

AM is a potent vasodilator peptide that was originally isolated from human pheochromocytoma.[1] There are abundant binding sites for AM in the pulmonary vasculature.[10] The plasma AM level increases in proportion to the severity of pulmonary hypertension, and circulating AM is partially metabolized in the lungs.[11] Recently, we have shown that intravenous administration of AM significantly decreases pulmonary vascular resistance in patients with heart failure or primary pulmonary hypertension.[12,13] These findings suggest that AM plays an important role in the regulation of pulmonary vascular tone. Thus, we hypothesized that transplantation of AM DNA-transduced EPCs would improve monocrotaline (MCT)-induced pulmonary hypertension. To test this hypothesis, we investigated whether EPCs phagocytose DNA-gelatin complexes, which would allow nonviral gene transfer into EPCs; whether intravenously administered EPCs are incorporated into the pulmonary vasculature; and whether transplantation of AM DNA-transduced EPCs ameliorates MCT-induced pulmonary hypertension and improves survival in MCT rats.

Methods

Culture of EPCs

Human umbilical cord blood mononuclear cells were plated on fibronectin-coated dishes and cultured in Medium 199 supplemented with 20% FBS, bovine pituitary extract, vascular endothelial growth factor, basic fibroblast growth factor, heparin, and antibiotics, as reported previously.[3,6,14] On days 4 and 8 of culture, nonadherent cells were removed, and medium was replaced. All mothers gave written informed consent, and the study was approved by the ethics committee.

Fluorescent Staining for EPCs

Adherent cells on day 8 of culture were stained by acetylated LDL labeled with DiI (DiI-acLDL, Biomedical Technologies) and fluorescein isothiocyanate (FITC)-labeled lectin from ulex europaeus (Sigma). Double-positive cells for DiI-acLDL and FITC-labeled lectin were identified as EPCs, as reported previously.[15,16]

Flow Cytometry

Adherent cells on day 8 of culture and green fluorescent protein (GFP) gene-transduced cells were analyzed by fluorescence-activated cell sorting (FACS; FACS SCAN flow cytometer, Becton Dickinson). Cells were incubated for 30 minutes at 4°C with phycoerythrin-conjugated mouse monoclonal antibodies against human CD14 (clone M5E2), CD31 (clone L133.1), CD68 (clone Y1/82A), and CD83 (clone HB15e; all from Becton Dickinson) and mouse monoclonal antibodies against human KDR (clone KDR-1, Sigma) and VE-cadherin (clone BV6, Chemicon). Isotype-identical antibodies served as controls.

Preparation of Biodegradable Gelatin and Plasmid DNA

We prepared biodegradable cationic gelatin, as a matrix to hold plasmid DNA, as reported previously.[7] In brief, a gelatin sample with an isoelectric point of 9.0 was isolated from bovine bone collagen. Gelatin microspheres were prepared through the glutaraldehyde cross-linking of gelatin. The microspheres were washed with acetone and distilled water and then freeze-dried. We constructed the pcDNA1.1-CMV vector (Invitrogen) encoding human AM cDNA or GFP cDNA. The gelatin (5 to 30 μm in diameter, 2 mg) was added to plasmid DNA (200 μg/200 μL in PBS, pH 7.4). After 24-hour incubation at 4°C, DNA-gelatin complexes were obtained.

Ex Vivo Gene Transfer Into EPCs

EPCs (5×10^5) were cultured with ionically linked GFP or AM DNA-gelatin complexes (200 μg/2 mg) for 72 hours. To examine DNA localization, AM plasmid DNA was labeled by rhodamine B isothiocyanate (RITC), as reported previously.[8] The nuclei of EPCs were stained by DAPI (Sigma). Immunocytochemistry for AM was performed with a mouse monoclonal antibody against human AM-(46-52). Human AM level in culture medium (n=5) was measured by radioimmunoassay.

Assay for AM

The culture medium and lung tissues were acidified with acetic acid, boiled to inactivate intrinsic proteases, and lyophilized. Human AM levels in culture medium, lung tissues, and plasma were measured with a radioimmunoassay kit (Shionogi).[12]

In Vivo Experimental Protocol

Male immunodeficient (F344/N rnu/rnu) nude rats weighing 100 to 120 g were randomly assigned to receive a subcutaneous injection of 60 mg/kg MCT or 0.9% saline. Seven days after MCT injection, 1×10^6 EPCs, 1×10^6 AM-expressing EPCs, or culture medium (500 μL each) was administered intravenously via the left jugular vein. Sham rats also received intravenous administration of 500 μL of culture medium. We used 1×10^6 cells per rat to obtain maximal effects of transplanted EPCs on the basis of dose-response experiments. This protocol resulted in the creation of 4 groups: MCT rats given EPCs (EPC group, n=8), MCT rats given AM-expressing EPCs (AM-EPC group, n=9), MCT rats given culture medium (control group, n=9), and sham rats given culture medium (sham group, n=8). Human mature pulmonary artery endothelial cells served as control cells.

Hemodynamic studies were performed 3 weeks after MCT injection. A polyethylene catheter was inserted into the right femoral artery. An umbilical vessel catheter was inserted through the right jugular vein into the pulmonary artery. Cardiac output was measured in triplicate by the thermodilution method. Pulmonary vascular resistance was calculated by dividing mean pulmonary arterial pressure by cardiac output.

Immunohistochemical and Immunofluorescence Staining

Immunohistochemistry was performed on paraformaldehyde-fixed, paraffin-embedded 5-μm sections of the lungs. To discern human endothelial cells from rat cells, we used mouse anti-human CD31 (DAKO) and mouse anti-rat CD31 (BD PharMingen) monoclonal antibodies. The sections were sequentially developed for the peroxidase and alkaline phosphatase substrates. Immunofluorescence staining for rat CD31 was performed on frozen sections with mouse anti-rat CD31 monoclonal antibody (BD PharMingen) and RITC-conjugated anti-mouse IgG antibody (DAKO).

Morphometric Analysis of Pulmonary Arteries

We analyzed the medial wall thickness of the pulmonary arteries in the middle region of the right lung (20 muscular arteries/rat, ranging in external diameter from 25 to 50 and from 51 to 100 μm). The medial wall thickness was expressed as follows: % wall thickness=[(medial thickness×2)/external diameter]×100.

Survival Analysis

Seven days after MCT injection, 29 rats received intravenous injection of 1×10^6 EPCs (EPC group, n=10), 1×10^6 AM-expressing EPCs (AM-EPC group, n=10), or culture medium (control group, n=9). Survival was estimated from the date of MCT injection to the death of the rat or 10 weeks after transplantation.

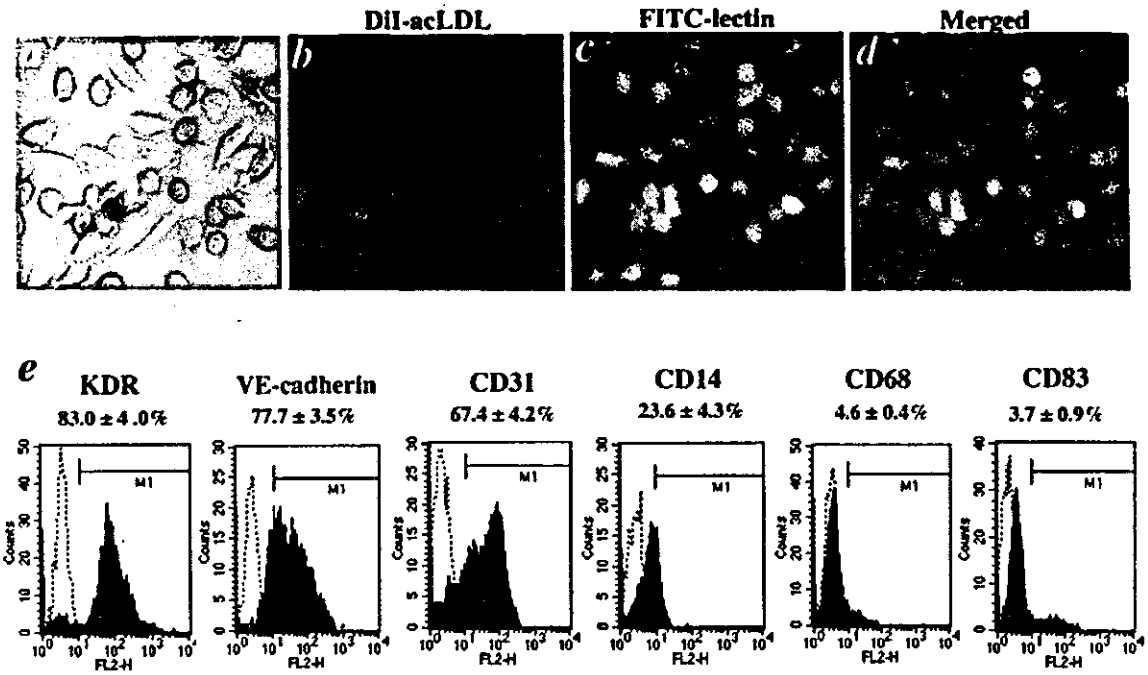

Figure 1. Characterization of EPCs derived from human umbilical cord blood. EPCs exhibited spindle-shaped or cobblestone-like morphology (a) and took up Dil-acLDL and FITC-labeled lectin in same field (b–d). e, Flow cytometric analysis of adherent cells on day 8. Most of adherent cells expressed endothelial lineage markers (KDR, VE-cadherin, and CD31), whereas they were negative for CD68 and CD83.

Statistical Analysis

Data were expressed as mean±SEM. Comparisons of parameters among the 4 groups were made by 1-way ANOVA, followed by the Scheffe multiple comparison test. Comparisons of the time course of parameters between the 2 groups were made by 2-way ANOVA for repeated measures, followed by the Scheffe multiple comparison test. Survival curves were derived by the Kaplan-Meier method and compared with log-rank tests. A probability value <0.05 was considered statistically significant.

Results

EPCs From Human Umbilical Cord Blood

After 8-day culture of mononuclear cells, spindle-shaped or cobblestone-like adherent cells were observed (Figure 1a). Most of the adherent cells were double stained by DiI-acLDL and FITC-labeled lectin (Figure 1b, c, and d). These cells expressed endothelial cell–specific antigens (KDR, VE-cadherin, and CD31; Figure 1e). In contrast, the majority of adherent cells were negative for monocyte/macrophage marker CD68 and dendritic cell marker CD83. Although a small fraction of the adherent cells expressed monocyte marker CD14, this marker has been shown to also be expressed on activated endothelial cells and cultured EPCs.[17] Thus, we confirmed that the major population of the adherent cells were EPCs.

Phagocytosis of DNA-Gelatin Complex by EPCs

EPCs were cultured with GFP DNA-gelatin complexes (Figure 2a). Interestingly, GFP was expressed in EPCs after 72-hour incubation (Figure 2b). Quantitative analyses by FACS confirmed a high incidence (76±3%, n=5) of GFP expression in adherent cells. KDR/GFP double-positive cells made up 70±2% of the adherent cells, whereas CD68/GFP double-positive cells accounted for 2±1% (Figure 2c). Transmission electron microscopy demonstrated that EPCs were phagocytosing DNA-gelatin complexes (Figure 2d). These results suggest that EPCs phagocytose DNA-gelatin complexes in coculture, which allows nonviral, highly efficient gene transfer into EPCs. Unlike gelatin, cationic liposome-mediated transfection efficiency was low (24±3%).

A number of DNA particles labeled by RITC were incorporated into gelatin (Figure 2e). RITC-labeled DNA particles were gradually released from gelatin within EPCs through gelatin degradation (Figure 2f). After 72-hour incubation, RITC-labeled DNA particles released from gelatin were distributed in the cytoplasm of EPCs (Figure 2g). These results suggest the ability of EPCs to take up DNA-gelatin complexes and dissolve the gelatin, freeing the DNA into EPCs. Unlike EPCs, human mature pulmonary artery endothelial cells did not phagocytose DNA-gelatin complexes.

When EPCs were cultured with AM DNA-gelatin complexes, intense immunostaining for AM was observed in EPCs impregnated with AM DNA-gelatin (Figure 3a). After 72-hour incubation, EPCs markedly secreted AM into the culture medium (10-fold increase compared with EPCs alone; Figure 3b). AM overproduction lasted for more than 16 days after gene transfer. AM secretion from EPCs was not influenced by the presence of gelatin (data not shown).

Incorporation of EPCs Into the Pulmonary Vasculature

GFP-expressing EPCs were administered intravenously 7 days after MCT injection. Three days after transplantation,